









Research Article

Modelling the Transmission Dynamics of Meningitis among High and Low-Risk People in Ghana with Cost-Effectiveness Analysis

Nicholas Kwasi-Do Ohene Opoku , Reindorf Nartey Borkor , Andrews Frimpong Adu , Hannah Nyarkoah Nyarko , Albert Doughan , Edwin Moses Appiah , Biigba Yakubu , Isabel Mensah , and Samson Pandam Salifu 

Kwame Nkrumah University of Science and Technology, Ghana

Correspondence should be addressed to Nicholas Kwasi-Do Ohene Opoku; nicholas@aims.edu.gh and Samson Pandam Salifu; sspandam@knust.edu.gh

Received 5 April 2022; Revised 27 October 2022; Accepted 2 November 2022; Published 21 November 2022

Academic Editor: Victor Kovtunenکو

Copyright © 2022 Nicholas Kwasi-Do Ohene Opoku et al. This is an open access article distributed under the Creative Commons Attribution License, which permits unrestricted use, distribution, and reproduction in any medium, provided the original work is properly cited.

Meningitis is an inflammation of the meninges, which covers the brain and spinal cord. Every year, most individuals within sub-Saharan Africa suffer from meningococcal meningitis. Moreover, tens of thousands of these cases result in death, especially during major epidemics. The transmission dynamics of the disease keep changing, according to health practitioners. The goal of this study is to exploit robust mechanisms to manage and prevent the disease at a minimal cost due to its public health implications. A significant concern found to aid in the transmission of meningitis disease is the movement and interaction of individuals from low-risk to high-risk zones during the outbreak season. Thus, this article develops a mathematical model that ascertains the dynamics involved in meningitis transmissions by partitioning individuals into low- and high-risk susceptible groups. After computing the basic reproduction number, the model is shown to exhibit a unique local asymptotically stability at the meningitis-free equilibrium \mathcal{E}_+ , when the effective reproduction number $R_0 < 1$, and the existence of two endemic equilibria for which $R_0^* < R_0 < 1$ and exhibits the phenomenon of backward bifurcation, which shows the difficulty of relying only on the reproduction number to control the disease. The effective reproductive number estimated in real time using the exponential growth method affirmed that the number of secondary meningitis infections will continue to increase without any intervention or policies. To find the best strategy for minimizing the number of carriers and infected individuals, we reformulated the model into an optimal control model using Pontryagin's maximum principles with intervention measures such as vaccination, treatment, and personal protection. Although Ghana's most preferred meningitis intervention method is via treatment, the model's simulations demonstrated that the best strategy to control meningitis is to combine vaccination with treatment. But the cost-effectiveness analysis results show that vaccination and treatment are among the most expensive measures to implement. For that reason, personal protection which is the most cost-effective measure needs to be encouraged, especially among individuals migrating from low- to high-risk meningitis belts.

1. Introduction

Meningitis is an inflammation of the meninges, which covers the brain and spinal cord [1]. It is a viral, fungal, or bacterial infection [1]. Although several bacterial infections cause meningitis, the trio, *Neisseria meningitidis* (*N. meningitidis*), *Streptococcus pneumoniae* (*S. pneumoniae*), and *Haemophilus influenzae* (*H. influenzae*) type B, are responsible for approximately 80% of all instances of bacterial meningitis [2]. The bacterium *Neisseria meningitidis* causes

meningococcal meningitis and is transmitted from one person to another via respiratory or pharyngeal secretions [2]. In West Africa, meningococcal meningitis is the most common form of bacterial meningitis, particularly in infants and children [3]. The disease's primary symptoms include headache, fever, stiff neck, vomiting, and sensitivity to light [4, 5]. According to the World Health Organization (WHO), as cited in [6], the incubation period of meningococcal meningitis varies between 2 and 10 days. The bacteria are commonly inhabited in the throat in about 11 to 25% of the population [6]. Hence, it is

possible for individuals infected with meningitis to show no symptoms; this is called the carriage state [5]. The management of bacterial meningitis includes preventive (vaccine usage) or curative (treatment with antibiotics) approach. However, no amount of treatment can prevent death by meningitis if diagnosed late [7]. Even with early detection, about 5 to 10% of these patients die within 24 to 48 hours after the onset of symptoms [7].

Globally, more than 1.2 million bacterial meningitis cases are reported yearly, and mortality rates of the disease differ by location, nation, pathogen, and age group [8]. According to the World Health Organization, the yearly worldwide incidence of pneumococcal meningitis is between 1000 and 2000 cases per 100000 people [8]. Meningitis is most common in what is known as the “meningitis belt” in sub-Saharan Africa, which stretches from Senegal to Ethiopia [8]. Seasonal outbreaks occur during the dry season (from January to April) [8]. The dry winds of the Harmattan blowing over the western part of Africa carry dust and sand particles with them, a situation that promotes the infection rate [8]. Individuals living within the dry belt are mostly affected by the dry winds which irritate the mucous membranes of their upper respiratory system, making them prone to the meningitis infection. The sub-Saharan Africa region annually reports approximately 10,000 deaths due to meningococcal meningitis [8]. Figure 1 depicts the case scenario of meningitis in sub-Saharan Africa.

The northern part of Ghana is within the African meningitis belt, with the highest prevalence of meningitis globally [10–13]. In Ghana, the belt encompasses the northern, the upper east, the upper west, and northern portions of the Brong Ahafo and Volta Regions [14]. *N. meningitidis* serogroups A, C, and, recently, W have produced large-scale epidemics in Ghana and other countries within the meningitis belt; *S. pneumoniae* outbreaks have also been reported in countries within this area [14]. Between 2010 and 2015, Ghana recorded 3000 cases of meningitis and 400 fatalities [15]. Meningococcal meningitis accounts for more than 95% of Ghana’s meningitis cases.

Bacterial meningitis spreads with the aid of environmental variables such as climate change and rainfall patterns, low absolute humidity, and dust [11]. According to the WHO, travelling or migration also aids in the spread of meningitis [16, 17]. Moreover, inaccurate diagnosis, overcrowding, coughing and sneezing, sharing of belongings, secondhand smoke exposure, and poor sanitation cause high-risk pathogen carriage and transmission [18]. Early detection of the causative organism ensures better management, treatment, and effectively controlling the spread of the infection [19]. Additional interventional methods to prevent the spread of meningitis include large-scale immunization [20]. Ghana uses two meningitis vaccines, MenAfriVac and PCV13 [20]. Global Alliance for Vaccine and Immunization (Gavi) implemented the MenAfriVac and PCV13 vaccines in the year 2012 in Ghana [20]. The PCV13 is administered in the national childhood vaccination programme, three doses to neonates at 6, 10, and 14 weeks.

In contrast, the MenAfriVac is involved in vaccinating both children and adults [20]. Despite these interventions, meningitis epidemics continue to occur regularly throughout the meningitis belt. Thus, stakeholders continue to ask questions about how

to curb the transmission of meningitis infection. Several studies, most importantly, compartmental models, have been used as a benchmark tool for modelling the transmission dynamics of meningitis to ascertain its spread among individuals. For example, a study by [21] used an eight compartmental model to provide short-term disease control when the vaccine, MenAfriVac, was introduced and implemented at high stake. The study claimed a strong resurgence of the meningitis disease with no subsequent immunization. However, it was established that about 10 to 20% of infected people who survived meningitis via vaccination developed some form of disability [22]. In the treatment and vaccination model to assess the impact on meningitis transmission, it was shown that implementing both vaccination and treatment is the most effective strategy for limiting the transmission of meningitis disease [23]. While vaccination aids in developing long-term or short-term immunity in susceptible individuals, treatment lowers disease-related fatalities and the number of infectious persons within the population. However, it is worth to note that the transmission dynamics of meningitis are determined by the type of strains involved in the transmission. [24] developed a model that considered the multiple strain of the meningitis disease to understand its qualitative properties. Though they failed to incorporate the effect of vaccination on the strains, they provided a unique assessment of the meningitis situation in Nigeria. Incorporating an optimal control analysis, [25] studied the impact of vaccination in an endemic setting with a limited number of antibiotics and hospital beds. The work provided a potential framework for controlling the disease spread in limited-resource environments, yet it failed to fully identify the most cost-effective approach to help curb the transmission of meningitis disease.

Though several models explain the epidemiology of meningococcal meningitis in the African meningitis belt, limited studies have comprehensively examined the meningitis situation in Ghana. Moreover, the nature and dynamics of the disease keep changing, as reported by the WHO and the Center for Disease Control (CDC) suggest that additional novel models are needed to curb the disease. It has been shown that migration and individual lifestyle keeps posing a challenge to reducing disease transmission. Here, we constructed a novel meningococcal infection transmission model to contribute to this new development. We modify the model developed in [25] to incorporate the dynamics of both high- and low-risk migration individuals. Furthermore, using meningitis data from Ghana, we ascertain important elements such as optimal control, generation time sensitivity analysis, and cost-effectiveness strategies. To the best of our knowledge, this study is the first work to uniquely incorporate the transmission of meningococcal disease on low-risk individuals and assess the sensitivity analysis of the reproduction number using exponential growth rate and generation time in a meningitis study.

2. The Model

According to the CDC and WHO, meningitis transmission occurs when there is close or lengthy contact with a patient having the meningococcal disease [26]. These organizations further indicated that the risk ratio differs from one person to another. For example, long-term travelers to the

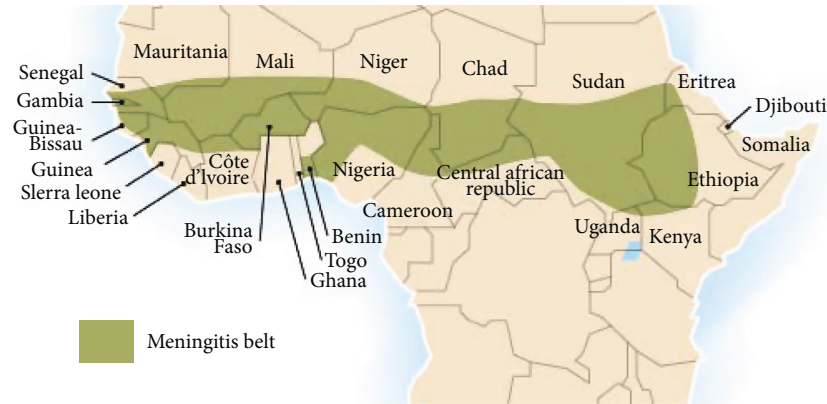


FIGURE 1: The meningitis belt of sub-Saharan Africa [9]. Meningitis is endemic within the belts, and outbreaks are facilitated by dry winds during the Harmattan season between January and April.

meningitis belt in sub-Saharan Africa may be at higher risk for meningococcal disease compared to travelers to nonmeningitis belt [26]. The WHO further noted that symptoms of meningitis usually appear between 4 and 10 days, causing most individuals to harbor the bacterium for weeks or even months without showing any clinical symptoms, a situation referred to as asymptomatic carriers [26]. According to [27], most meningitis cases are exposed to asymptomatic carriers, killing about 10% of infected individuals within a few hours. However, an individual can recover from the disease with early diagnosis and treatment [27].

Adopting the information and assertions provided by experts, we assumed five (5) mutually exclusive compartments to indicate individuals with unique natures. We group the population into subpopulations of high-risk susceptible individuals (S_H), low-risk susceptible individuals (S_L), carriers (asymptomatic infections) (C), infectious individuals (I), and recovered individuals (R). The susceptible compartment is assumed to increase through immigration or birth, collectively referred to as the recruitment rate and denoted by π . A fraction Δ of the recruited individuals are assumed to be at low risk, while the remaining fraction of $(1 - \Delta)$ is at high risk of being infected with the meningitis disease. The parameter β represents effective contact rate between carriers, infected individuals, and the susceptible population. However, the rate of infection probability differs between infected and carriers. Thus, the per capita infection rate by infected and carrier individuals is represented by ω_1 and ω , respectively. Therefore, the force of new infections is given by

$$\lambda = \frac{\beta(\omega C + \omega_1 I)}{N}. \tag{1}$$

Equation (1) indicates the standard incidence rate of new infections. It is normalized by the total population $N = S_H + S_L + C + I + R$. However, the risk effect of individuals in S_L compartment is further assumed to be infected at a reduced rate $(1 - a)$, where $a \in [0, 1]$ measures the modification behavior of the low-risk individuals. If $a = 0$, it implies a negative modification behavior by low-risk individuals, increasing their

chances of being infected with the disease. Examples of these negative modification behaviors include large group gathering, traveling to the meningitis belt in sub-Saharan Africa during the dry season, etc. But, if $a = 1$, it implies that low-risk individuals have a positive modification behavior which helps prevent them from meningitis infection. After elapsing the incubation period, which is the time from infection to onset of symptoms, we assume that an individual moves from carrier to the infected compartment at the rate σ . Both individuals in the carrier and infected compartments recover from meningitis disease at a rate η_2 and η_1 , respectively. In contrast, a natural death rate denoted by μ occurs in all the compartments while disease-induced mortality is denoted by d . It is reported by the WHO and CDC that though it is very unusual for anyone to have meningitis more than once, it is possible. Moreover, some people develop immunity to the specific organism that has caused their disease. But because there are several different causes of meningitis, it is therefore possible, but rare, to have the disease more than once. Based on this assertion, we further assume that a proportion of individuals denoted by θ and $1 - \theta$ loss their immunity and either become low- or high-risk susceptible individuals to other types or strain of the meningitis disease, respectively. Figure 2 shows the compartmental diagram of the proposed deterministic model.

The model assumptions give rise to the following system of differential equations:

$$\begin{aligned} \frac{dS_H}{dt} &= (1 - \Delta)\pi - \lambda S_H - \mu S_H + (1 - \theta)\xi, \\ \frac{dS_L}{dt} &= \Delta\pi - (1 - a)\lambda S_L - \mu S_L + \theta\xi, \\ \frac{dC}{dt} &= \lambda S_H + (1 - a)\lambda S_L - (\eta_2 + \sigma + \mu)C, \\ \frac{dI}{dt} &= \sigma C - (\eta_1 + \mu + d)I, \\ \frac{dR}{dt} &= \eta_2 C + \eta_1 I - (\theta\xi + (1 - \theta) + \mu)R. \end{aligned} \tag{2}$$

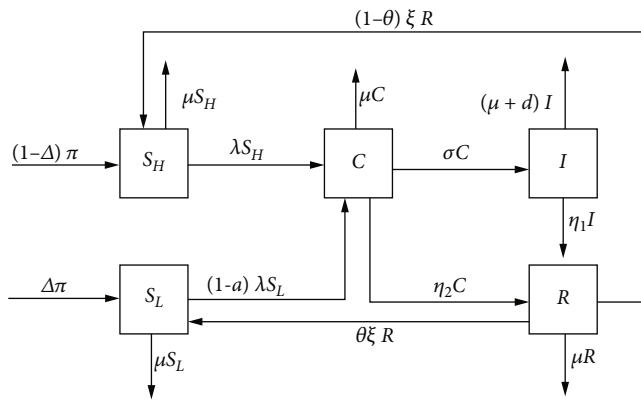


FIGURE 2: Schematic diagram of the low- and high-risk susceptible-carrier-infected-recovered (SCIR) model depicting meningitis transmissions between different compartments. The five squares represent the compartments of individuals while the movement between the compartments is indicated by the black arrows.

3. Model Dynamics

3.1. Positivity and Boundedness of Solutions. Theoretically, because the system (2) describes an epidemic disease in a human population, parameters of the stated model must be nonnegative. To make the system (2) epidemiologically meaningful, we show that the state variables are nonnegative. The system (2) is well posed when the system starts with nonnegative initial conditions $(S_H(0), S_L(0), C(0), I(0), R(0))$; then, the solutions of the system (2) will remain nonnegative for all $t \in [0, \hat{t})$ and that these positive solutions are bounded. We thus apply the following theorem.

Theorem 1 (positivity of solution). *Given that the $S_H(0) > 0$, $S_L(0) > 0$, $C(0) \geq 0$, $I(0) \geq 0$, $R(0) \geq 0$, and $\lambda > 0$, then the solutions $S_H(t), S_L(t), C(t), I(t), R(t)$ of the system (2) will always be nonnegative.*

Proof. We define

$$\hat{t} = \sup \{t > 0; S_H(t) \geq 0, S_L(t) \geq 0, C(t) \geq 0, I(t) \geq 0, R(t) \geq 0\}. \quad (3)$$

Clearly, $\hat{t} > 0$, hence suppose that $S_L(0) \geq 0$ then the second equation of the system (2) leads to

$$\frac{dS_L}{dt} = \Delta\pi + \theta\xi - (1-a)\lambda S_L - \mu S_L. \quad (4)$$

Since $\Delta\pi, \theta\xi$ are positive; we have

$$\begin{aligned} \frac{dS_L}{dt} &\geq -(1-a)\lambda S_L - \mu S_L, \\ \int_0^{\hat{t}} \frac{dS_L}{S_L} &\geq \int_0^{\hat{t}} -((1-a)\lambda + \mu) dt, \\ S_L(\hat{t}) &\geq S_L(0) e^{-((1-a)\lambda + \mu)\hat{t}} \geq 0. \end{aligned} \quad (5)$$

Similarly, the first equation of system (2)

$$\begin{aligned} \frac{dS_H}{dt} &\geq -(\lambda + \mu)S_H, \\ \frac{dS_H}{S_H} &\geq -(\lambda + \mu)dt. \end{aligned} \quad (6)$$

Integrating both sides from $t = 0, t = \hat{t}$, we obtain

$$\begin{aligned} \int_0^{\hat{t}} \frac{dS_H}{S_H} &\geq -\int_0^{\hat{t}} (\lambda + \mu) dt, \\ S_H(\hat{t}) &\geq S_H(0) e^{-((\lambda + \mu)\hat{t})} \geq 0, \end{aligned} \quad (7)$$

and using the Gronwall inequality, the solution for C, I , and R becomes

$$\begin{aligned} C(\hat{t}) &\geq C(0) e^{-(\eta_2 + \sigma + \mu)\hat{t}} \geq 0, \\ I(\hat{t}) &\geq I(0) e^{-(\eta_1 + \mu + d)\hat{t}} \geq 0, \\ R(\hat{t}) &\geq R(0) e^{-(\theta\xi + (1-\theta)\xi + \mu)\hat{t}} \geq 0, \end{aligned} \quad (8)$$

respectively. \square

Next, we prove the boundedness of solutions for the system (2) using the following theorem.

Theorem 2 (boundedness of solution). *All solutions (S_H, S_L, C, I, R) of system (2) are bounded.*

Proof. The total population denoted by N is defined as

$$N(t) = S_H(t) + S_L(t) + C(t) + I(t) + R(t). \quad (9)$$

Differentiating Equation (9) gives

$$\frac{dN}{dt} = \frac{dS_H}{dt} + \frac{dS_L}{dt} + \frac{dC}{dt} + \frac{dI}{dt} + \frac{dR}{dt}. \quad (10)$$

It follows from Equation (10) that

$$\frac{dN}{dt} = \pi - \mu N. \quad (11)$$

Applying Gronwall's inequality, the solution for Equation (11) becomes

$$N(t) = \frac{\pi}{\mu} + \left(N(0) - \frac{\pi}{\mu}\right) e^{-\mu t}. \quad (12)$$

Thus, $N(t) = \pi/\mu \forall t > 0$ whenever $N(0) \leq \pi/\mu$. It is trivial to see that $\lim_{t \rightarrow +\infty} \sup N \leq \pi/\mu$. \square

Clearly, $N(t)$ and all variables of the system (2) are bounded, and it will be analyzed in the biologically feasible region given by

$$\Omega = \left\{ (S_H, S_L, C_I, R) \in \mathcal{R}_+^5, N(t) \leq \frac{\pi}{\mu}, S_H(t) \geq 0, S_L(t) \geq 0, C(t) \geq 0, I(t) \geq 0, R(t) \geq 0 \right\}. \tag{13}$$

Equation (13) shows that system (2) exists in the positive orthant \mathcal{R}_+^5 which eventually enters and remains in the attracting subset Ω . Therefore, the set Ω is made up of the local and global attractor of the system (2). Thus, the set $\Omega \subset \mathcal{R}_+^5$ is compact, positively invariant, and attracting with respect to the system (2).

3.2. Meningitis-Free Equilibrium (\mathcal{E}_+). The meningitis-free equilibrium (MFE) corresponds to the situation where no meningococcal disease exists in the system. Thus, if $I = 0$, then $C = R = 0$. Hence, the solution for meningitis-free equilibrium point is

$$\left(S_{H_+}, S_{L_+}, C_+, I_+, R_+ \right) = \left(\frac{(1-\Delta)\pi}{\mu}, \frac{\Delta\pi}{\mu}, 0, 0, 0 \right). \tag{14}$$

3.3. Basic Reproduction Number. The basic reproduction number is the number of new meningitis infections generated from one carrier or infected individual in a susceptible or disease-free population [28]. It is denoted by R_0 . To compute the R_0 of the system (2), we use the next-generation method applied in [29] by considering only the infectious classes, that is, C and I . A good rule of thumb requires computing the F and V matrices, which denotes the rate of appearances of new infections in the infected compartments and the transfer of individuals into and out of the infected compartment. From the system (2), we derived the matrices F and V as follows:

$$\mathcal{F} = \begin{bmatrix} \beta\omega(1-\Delta) + \beta\omega(1-a)\Delta & \beta\omega_1(1-\Delta) + \beta\omega_1\Delta(1-a) \\ 0 & 0 \end{bmatrix},$$

$$\mathcal{V} = \begin{bmatrix} \eta_2 + \sigma + \mu & 0 \\ -\sigma & \eta_1 + \mu + d \end{bmatrix}. \tag{15}$$

The spectral radius of $\mathcal{F}\mathcal{V}^{-1}$ given by $R_0 = \rho(\mathcal{F}\mathcal{V}^{-1})$ is obtained as

$$R_0 = \frac{(\beta\Delta\omega(1-a) + \beta\omega(1-\Delta))(\eta_1 + \mu + d) + \beta\Delta\omega_1\sigma(1-a) + \beta\omega_1\sigma(1-\Delta)}{(\eta_2 + \mu + \sigma)(\eta_1 + \mu + d)}. \tag{16}$$

Equation (16) shows that the basic reproduction number is the sum of two infectious terms, i.e., carriers and infected meningitis individuals from the high- and low-risk compartments. Further, for $\beta = 0$, we have $R_0 = 0$, which denotes the meningitis-free state of the infection. Moreover, for $\sigma = 0$, it implies that no one progresses to the infected compartment; thus, we only have carrier individuals within the system. The WHO indicates that about 5-25% of individuals might have the bacteria in their nose or throat without showing any sign of being sick but are still infectious to others. Exposure to these asymptomatic carriers causes most meningitis cases, as seen from the terms in Equation (16).

3.4. Local Stability of MFE. This section analyzes the system's stability by constructing a Jacobian matrix and finding the corresponding characteristic equation. In epidemiological studies, it is a well-established fact that the basic reproduction number determines the trajectory of the meningitis-free equilibrium point. It is wholly because when $R_0 < 1$, an individual infected with the meningitis infection generates fewer than one new infected person during the period of its infection and vice versa. We apply the following theorem.

Theorem 3. *The MFE, \mathcal{E}_+ , of the system (2), is locally-asymptotically stable (LAS) in Ω if $R_0 < 1$ and unstable if $R_0 > 1$.*

Proof. The Jacobian matrix of the system (2) at the MFE point is given by

$$J_{\mathcal{E}_+} = \begin{bmatrix} -\mu & 0 & 0 & 0 & 0 \\ 0 & -\mu & 0 & 0 & 0 \\ 0 & 0 & \beta\omega(S_{H_+} + (1-a)S_{L_+}) - (\sigma + \eta_2 + \mu) & \beta\omega_1(S_{H_+} + S_{L_+}) & 0 \\ 0 & 0 & \sigma & -(\eta_1 + \mu + d) & 0 \\ 0 & 0 & \eta_2 & \eta_1 & -(\theta\xi + (1-\theta)\xi + \mu) \end{bmatrix}. \tag{17}$$

The eigenvalues of the Equation (17) are $\lambda_{1,2} = -\mu$ and $\lambda_5 = -(\theta\xi + (1-\theta)\xi + \mu)$, with the remaining two eigenvalues ($\lambda_{3,4}$) derived from the following submatrix of Equation (17).

$$J_{\mathcal{E}_t}^1 = \begin{bmatrix} \beta\omega(S_{H_t} + (1-a)S_{L_t}) - (\sigma + \eta_2 + \mu) & \beta\omega_1(S_{H_t} + S_{L_t}(1-a)) \\ \sigma & -(\eta_1 + \mu + d) \end{bmatrix}. \quad (18)$$

The meningitis-free equilibrium is locally stable if the eigenvalues of Equation (18) are negative. All eigenvalues in Equation (18) are negative if and only if the trace of $J_{\mathcal{E}_t}^1 < 0$ and the determinant of $J_{\mathcal{E}_t}^1 > 0$. From Equation (18), we obtained the characteristic polynomial as

$$Z^2 + \lambda_4 Z + \lambda_5 = 0, \quad (19)$$

where

$$\begin{aligned} \lambda_3 &= \beta\omega(1-\Delta) + \beta\omega(1-a)\Delta - (\sigma + \eta_2 + \mu) - (\eta_1 + \mu + d) \\ &= R_0(\eta_1 + \mu + d)(\eta_2 + \mu + \sigma) - (\beta\omega_1\Delta\sigma(1-a) + \beta\omega_1\sigma(1-\Delta)) \\ &\quad - (\sigma + \eta_2 + \mu)^2 - (\eta_1 + \mu + d)(\eta_2 + \mu + \sigma) \\ &= (R_0 - 1)(\eta_1 + \mu + d)(\eta_2 + \mu + \sigma) - (\sigma + \eta_2 + \mu)^2 \\ &\quad - (\beta\omega_1\Delta\sigma(1-a) + \beta\omega_1\sigma(1-\Delta)), \end{aligned} \quad (20)$$

$$\begin{aligned} \lambda_4 &= -(\eta_1 + \mu + d)(\beta\omega(1-\Delta) + \beta\omega(1-a)\Delta - (\sigma + \eta_2 + \mu)) \\ &\quad - (\sigma(\beta\omega_1(1-\Delta) + \beta\omega_1(1-a)\Delta)) \\ &= -R_0(\eta_1 + \mu + d)(\eta_2 + \mu + \sigma) + (\eta_1 + \mu + d)(\eta_2 + \mu + \sigma) \\ &= (\eta_1 + \mu + d)(\eta_2 + \mu + \sigma)(1 - R_0). \end{aligned} \quad (21)$$

Equation (20) shows that the trace of (18) is negative while the determinant (as shown in Equation (21)) is positive if and only if $R_0 < 1$. Thus, the meningitis-free equilibrium is locally stable if $R_0 < 1$. \square

3.5. Endemic Equilibrium Points \mathcal{E}^{} .** The endemic equilibrium point, $\mathcal{E}^{**} = \{S_H^{**}, S_L^{**}, C^{**}, I^{**}, R^{**}\}$, is derived by equating the right-hand terms of the system (2) to zero. Expressing all the variables in terms of the force of infection (λ), we get

$$\begin{aligned} S_H^{**} &= \frac{\pi(1-\Delta) + \xi(1-\theta)}{\lambda^{**} + \mu}, \\ S_L^{**} &= \frac{\pi\Delta + \theta\xi}{\lambda^{**}(1-a) + \mu}, \\ C^{**} &= \frac{\lambda^{**}((1-a)\pi\lambda^{**} + \pi(1-a\Delta)\mu + (1-a)\lambda^{**}\xi + (1-a\theta)\mu\xi)}{((1-a)\lambda^{**} + \mu)(\lambda^{**} + \mu)(\mu + \sigma + \eta_2)}, \\ I^{**} &= \frac{\lambda^{**}\sigma((1-a)\pi\lambda^{**} + \pi(1-a\Delta)\mu + (1-a)\lambda^{**}\xi + (1-a\theta)\mu\xi)}{((1-a)\lambda^{**} + \mu)(\lambda^{**} + \mu)(\mu + \xi)(d + \mu + \eta_1)(\mu + \sigma + \eta_2)}, \\ R^{**} &= \frac{\lambda^{**}((1-a)\pi\lambda^{**} + \pi(1-a\Delta)\mu + (1-a)\lambda^{**}\xi + (1-a\theta)\mu\xi)(\sigma\eta_1 + (d + \mu + \eta_1)\eta_2)}{((1-a)\lambda^{**} + \mu)(\lambda^{**} + \mu)(\mu + \xi)(d + \mu + \eta_1)(\mu + \sigma + \eta_2)}. \end{aligned} \quad (22)$$

TABLE 1: Number of possible positive roots of system (2).

B_0	B_1	B_2	Number of positive roots
+	+	+	0
-	+	+	1
-	-	+	1
+	-	+	2 or 0

The solutions for existence of the endemic equilibrium points are in two categories such that:

- (i) Category I: $\lambda^{\dagger\dagger} = 0$, which corresponds to the meningitis-free equilibrium point
- (ii) Category II: $\lambda^{\dagger\dagger} \neq 0$, which depicts the case in which there is the presence of the meningitis infection

The proof is completed by substituting the solutions of $C^{\dagger\dagger}$ and $I^{\dagger\dagger}$ into Equation (1). Using Mathematica v.13 to solve the system, we obtain the following polynomial:

$$B_2\lambda^{\dagger\dagger 2} + B_1\lambda^{\dagger\dagger} + B_0 = 0. \tag{23}$$

We define the variables in Equation (23) such that

$$\begin{aligned} B_2 &= (1 - a)\pi(\mu + \eta_1 + d)(\mu + \sigma + \eta_2), \\ B_1 &= -\mu((d + \mu + \eta_1)((2 - a)\pi(\mu + \sigma) + (1 - a)\beta\omega(\pi + \xi)) + (2 - a\pi\eta_2) + (1 - a)\beta\sigma\omega_1(\pi + \xi)), \\ B_0 &= \mu^2(\mu + \eta_1 + d)(\mu + \sigma + \eta_2)[1 - R_0]. \end{aligned} \tag{24}$$

Equation (24) shows that the coefficient of B_2 is always positive. However, if $B_0 < 0$ and $B_1^2 - 4B_2B_0 > 0$, then a unique endemic equilibrium exists irrespective of the sign of B_1 . Moreover, two positive real equilibrium points are obtained iff $B_0 > 0$, $B_1 < 0$, and $B_1^2 - 4B_2B_0 > 0$; otherwise, no endemic equilibrium point exists. The possibility of the existence of a backward bifurcation occurs when $B_0 > 0$, $B_1 < 0$, and $B_1^2 - 4B_2B_0 > 0$ in which the two endemic equilibria exist. Thus, the positive solutions of Equation (23) are

$$\lambda^{\dagger\dagger} = \frac{-B_1 \pm \sqrt{B_1^2 - 4B_2B_0}}{2B_2}. \tag{25}$$

To determine the threshold value of the reproduction number, R_0^\dagger , which is the value for which the MFE has a steady state, we derive

$$\begin{aligned} B_1^2 - 4B_2B_0 &= 0, \\ R_0^\dagger &= 1 - \frac{B_1^2}{4B_2(\mu^2)(\mu + \eta_1 + d)(\mu + \sigma + \eta_2)}. \end{aligned} \tag{26}$$

Therefore, the system (2) has two positive equilibria for which $R_0^\dagger < R_0 < 1$. The number of positive roots is summarized using Descartes' law of signs in Table 1.

3.6. Bifurcation Graph. Changes in a system's topological structure occur when the parameters within the system cross a critical point, a case scenario for a bifurcation phenomenon. The occurrence of bifurcation has important implications in public health studies because the system's behavior changes as the reproduction number passes the critical value of $R_0 = 1$. Thus, a backward bifurcation implies that just observing a positive behavior or obtaining a lower transmission or contact rate might not be enough to reduce R_0 below 1 to eliminate the meningitis disease. Hence, additional mea-

asures are needed to further reduce R_0 below R_0^\dagger to ensure the complete eradication of the disease.

Figure 3 shows changes within the system's qualitative behavior for $R_0 = 1$. When the value of $R_0 > 1$, it implies the persistence of meningitis disease within the population. A backward bifurcation (Figure 3(a)) exhibits the coexistence of both meningitis-free and endemic equilibrium state for values of R_0 between R_0^\dagger and 1. Thus, introducing additional control measures as explained in Section 4 is crucial.

3.7. Sensitivity Analysis of R_0 . As a result of the system behavior to the basic reproduction number, as shown in Subsection 3.6, we perform the sensitivity analysis of the reproduction ratio or number using supported estimation methods. We use the exponential growth method proposed by [30] to derive the generation time to estimate the initial basic reproduction number within the first 80 days of the meningitis epidemic in Ghana. The time lag between an infection in the primary and secondary cases is known as the "generation time" [30]. To compute the estimates of R_0 and generation time based on the exponential growth, we use readily available daily reported meningitis cases.

As shown in [30], we assumed that the number of newly recorded meningitis cases per day and generation time follows the Poisson and gamma distributions, respectively. Thus, if we denote the exponential growth rate by ξ , then the reproduction ratio is obtained as

$$R_0 = \frac{1}{\mathcal{M}(-\xi)}, \tag{27}$$

where \mathcal{M} represents the moment generating function of the discretized generation time distribution. The estimation of R_0 and generation time based on the exponential growth method for meningitis cannot be underrated since the estimate provides real-time information to quantify the impact

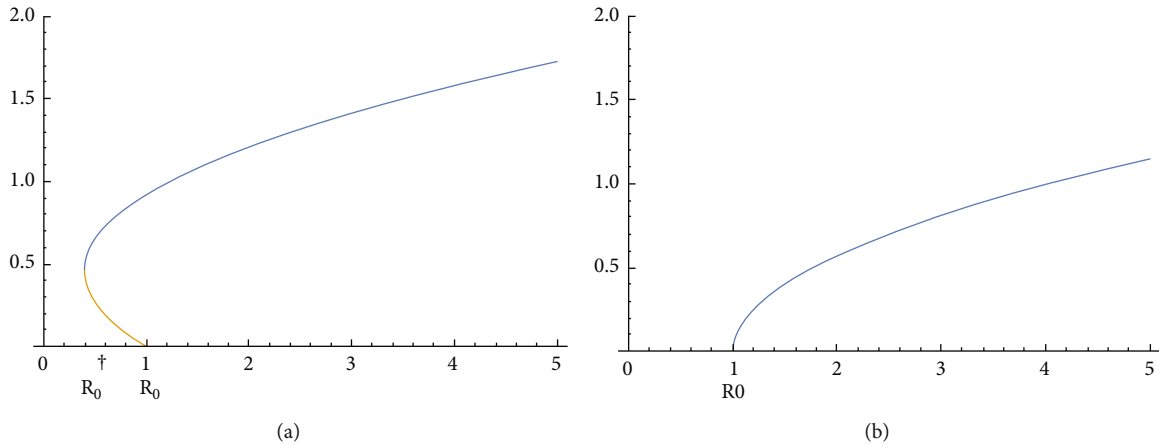


FIGURE 3: (a) Bifurcation diagram of system (2). The epidemiological importance of the existence of bifurcation especially a backward bifurcation in meningitis transmission model depicts that the classical requirement of having the basic reproduction number $R_0 < 1$, although necessary, is not sufficient for controlling the meningitis disease. (a) Backward bifurcation occurs in system (2) for $a = 0.25$ and $\beta = 0.4$, and (b) forward bifurcation will be achieved for $a = 0.87$ and $\beta = 0.004$.

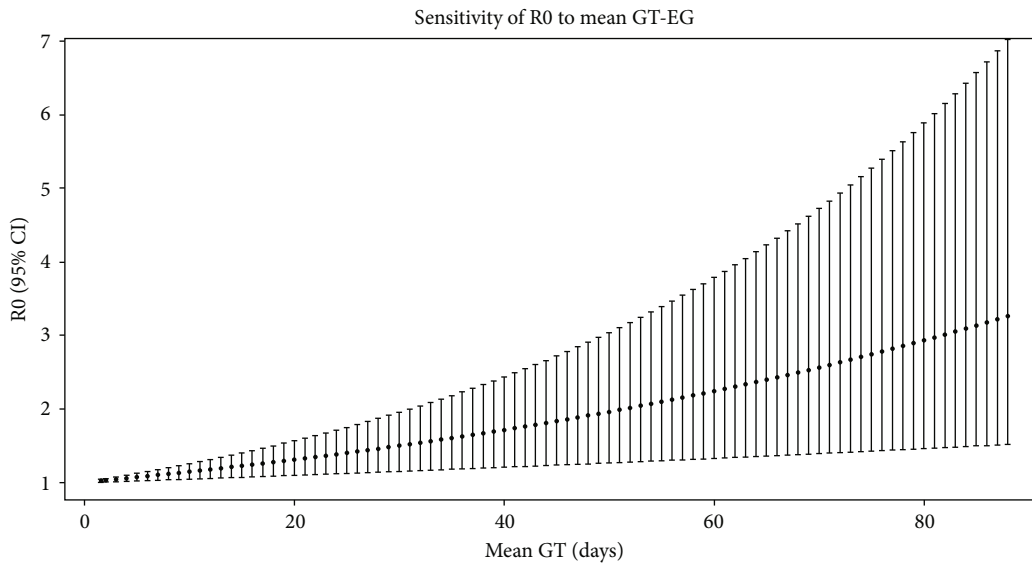


FIGURE 4: Sensitivity analysis of effective basic reproduction number and generation time (GT) using exponential growth (EG) estimate.

TABLE 2: Estimation of the initial reproductive number using exponential growth method and the variation in generation time (GT) from the initial day to the eighty-eighth day.

GT.Type	GT.Mean	GT.SD	R_0	CI.lower	CI.upper
Gamma	1.58	0.95	1.03	1.01	1.05
Gamma	2.04	1.01	1.03	1.012	1.057
Gamma	3.00	1.04	1.048	1.017	1.08
Gamma	4.00	1.04	1.06	1.02	1.10
Gamma	5.00	1.041	1.076	1.026	1.13

of necessary interventions to inform appropriate public health responses. Hence, the tool developed by [31], which sums up the exponential growth estimate process, is employed to derive Figure 4 and Table 2.

Figure 4 and Table 2 (see Table 3 for full table) show the variation of generation time from the initial day to the eighty-eighth day with a standard deviation of approximately 1. An increase in the R_0 estimates is observed between the

TABLE 3: Generation time and reproduction number estimates.

GT.Type	GT.Mean	GT.SD	R_0 estimates	CI.lower	CI.upper
Gamma	1.58087	0.9543	1.02812	1.0099	1.04663
Gamma	2.04095	1.00627	1.03446	1.01212	1.05726
Gamma	2.99986	1.03970	1.04780	1.01674	1.07980
Gamma	3.99989	1.04051	1.06190	1.02157	1.10384
Gamma	4.99995	1.04068	1.07619	1.02643	1.12842
Gamma	5.99956	1.03981	1.09067	1.03132	1.15353
Gamma	6.99968	1.04009	1.10536	1.03622	1.17921
Gamma	7.99975	1.04026	1.12023	1.04115	1.20546
Gamma	8.99980	1.04037	1.13531	1.04611	1.23230
Gamma	9.99984	1.04045	1.15059	1.05108	1.25974
Gamma	10.99986	1.04051	1.16608	1.05609	1.28778
Gamma	11.99988	1.04055	1.18178	1.06111	1.31645
Gamma	12.99989	1.04058	1.19768	1.06616	1.34576
Gamma	13.99990	1.04061	1.21380	1.07123	1.37572
Gamma	14.99991	1.04063	1.23014	1.07633	1.40634
Gamma	15.99992	1.04065	1.24670	1.08145	1.43765
Gamma	16.99992	1.04066	1.26348	1.08659	1.46966
Gamma	17.99993	1.04067	1.28049	1.09176	1.50238
Gamma	18.99993	1.04068	1.29772	1.09696	1.53582
Gamma	19.99994	1.04069	1.31519	1.10218	1.57001
Gamma	20.99994	1.04070	1.33289	1.10742	1.60496
Gamma	21.99994	1.04070	1.35083	1.11269	1.64069
Gamma	22.99995	1.04071	1.36901	1.11798	1.67722
Gamma	23.99995	1.04071	1.38744	1.12330	1.71456
Gamma	24.99995	1.04072	1.40612	1.12865	1.75273
Gamma	25.99995	1.04072	1.42504	1.13401	1.79174
Gamma	26.99995	1.04073	1.44422	1.13941	1.83164
Gamma	27.99996	1.04073	1.46366	1.14483	1.87241
Gamma	28.99996	1.04073	1.48336	1.15028	1.91410
Gamma	29.99997	1.04074	1.50333	1.15575	1.95671
Gamma	30.99996	1.04074	1.52356	1.16125	2.00027
Gamma	31.99996	1.04074	1.54407	1.16677	2.04480
Gamma	32.99996	1.04074	1.56485	1.17232	2.09032
Gamma	33.99996	1.04075	1.58591	1.17790	2.13686
Gamma	34.99996	1.04075	1.60726	1.18351	2.18443
Gamma	35.99996	1.04075	1.62889	1.18914	2.23306
Gamma	40.99997	1.04076	1.74151	1.21769	2.49294
Gamma	41.99997	1.04076	1.76495	1.22349	2.54843
Gamma	42.99997	1.04076	1.78870	1.22931	2.60517
Gamma	43.99997	1.04076	1.81278	1.23516	2.66316
Gamma	44.99997	1.04076	1.83718	1.24103	2.72245
Gamma	45.99997	1.04076	1.86191	1.24694	2.78306
Gamma	46.99997	1.04076	1.88697	1.25287	2.84502
Gamma	47.99997	1.04076	1.91237	1.25883	2.90835
Gamma	48.99997	1.04076	1.93811	1.26482	2.97311
Gamma	49.99997	1.04076	1.96419	1.27084	3.03929
Gamma	50.99997	1.04076	1.99063	1.27688	3.10695
Gamma	51.99997	1.04077	2.01743	1.28300	3.17611

TABLE 3: Continued.

GT.Type	GT.Mean	GT.SD	R_0 estimates	CI.lower	CI.upper
Gamma	52.99997	1.04077	2.04458	1.28906	3.24682
Gamma	53.99997	1.04077	2.07210	1.29520	3.31910
Gamma	54.99997	1.04077	2.10000	1.30136	3.39300
Gamma	55.99997	1.04077	2.12825	1.30755	3.46853
Gamma	56.99997	1.04077	2.15690	1.31377	3.54574
Gamma	57.99997	1.04077	2.18593	1.32002	3.62468
Gamma	58.99997	1.04077	2.21535	1.32630	3.70537
Gamma	59.99997	1.04077	2.24517	1.33261	3.78786
Gamma	60.99997	1.04077	2.27539	1.33895	3.87219
Gamma	61.99997	1.04077	2.30602	1.34532	3.95839
Gamma	62.99997	1.04077	2.33706	1.35172	4.04651
Gamma	63.99997	1.04077	2.36851	1.35815	4.13660
Gamma	64.99997	1.04077	2.40039	1.36461	4.22869
Gamma	65.99997	1.04077	2.43270	1.37111	4.32283
Gamma	66.99997	1.04077	2.46545	1.37763	4.41906
Gamma	67.99997	1.04077	2.49863	1.38418	4.51744
Gamma	68.99997	1.04077	2.53226	1.39077	4.61801
Gamma	69.99997	1.04077	2.56635	1.39739	4.72081
Gamma	70.99997	1.04077	2.60089	1.40403	4.82591
Gamma	71.99997	1.04077	2.63590	1.41071	4.93334
Gamma	72.99997	1.04077	2.67137	1.41743	5.04317
Gamma	73.99997	1.04078	2.70733	1.42417	5.15544
Gamma	74.99997	1.04078	2.74377	1.43094	5.27021
Gamma	75.99998	1.04078	2.78070	1.43775	5.38754
Gamma	76.99998	1.04078	2.81813	1.44460	5.50748
Gamma	77.99998	1.04078	2.85606	1.45147	5.63009
Gamma	78.99998	1.04078	2.89450	1.45837	5.75542
Gamma	79.99998	1.04078	2.93346	1.46531	5.88355
Gamma	80.99998	1.04078	2.97295	1.47228	6.01453
Gamma	81.99998	1.04078	3.01296	1.47929	6.14843
Gamma	82.99998	1.04078	3.05351	1.48632	6.28530
Gamma	83.99998	1.04078	3.09461	1.49339	6.42523
Gamma	84.99998	1.04078	3.13627	1.50050	6.56827
Gamma	85.99998	1.04078	3.17848	1.50764	6.71449
Gamma	86.99998	1.04078	3.22126	1.51481	6.86397
Gamma	87.99998	1.04078	3.26462	1.52202	7.01678

basic reproduction number and mean generation time for the exponential growth. The observation implies that without implementing an intervention programme, there will be a continuous increase in the number of secondary meningitis cases as the day goes by. Hence, to obtain a correct estimate of the average generation time and to make data driven policy decisions, there is an urgent need for more data on generation time or the introduction of robust intervention programmes to curb the meningitis disease.

4. Control Problem

This section accounts for the modification of system (2) into an optimal control problem. The linear function $q_i(t)$ for i

$= 1, 2, 3$ is defined such that the effectiveness of controls is achieved when $q_i(t) = 1$ and ineffective when $q_i(t) = 0$. In modifying system (2), the force of infection is reduced by the factor $(1 - q_1)$, where q_1 measures the effectiveness of incorporating vaccination. Moreover, the parameter q_2 represents the effectiveness of treatment as a control variable. As a rule of thumb, the CDC and WHO advise not to share items that aid the transmission of meningitis. Examples include water bottles, lip balm, toothbrushes, towels, drinking glasses, eating utensils, cosmetics, smoking materials, food, or drink from common sources. Experts in the health profession assert that implementing personal protection prevents the transmission of many, if not most, bacteria and viruses. Hence, the factor q_3 measures the level of success obtained due to prevention or personal protection. Using

the bounded Lebesgue measurable control, the set Q , which is the Lebesgue measurable, is defined by

$$Q = \{(q_1(t), q_2(t), q_3(t)) | 0 \leq q_i < q_{i \max} \leq 1 | \forall i = 1, 2, 3, t \in [0, T_F]\}, \tag{28}$$

and the objective function to be minimized is given as

$$J = \min_{q_1, q_2, q_3} \int_0^{T_F} \left(Z_1 C(t) + Z_2 I(t) + \frac{D_1}{2} q_1^2(t) + \frac{D_2}{2} q_2^2(t) + \frac{D_3}{2} q_3^2(t) \right) dt, \tag{29}$$

subject to the modified system

$$\begin{aligned} \frac{dS_H}{dt} &= (1 - \Delta)\pi - q_3 S_H - (1 - q_1)\lambda S_H - \mu S_H + (1 - \theta)\xi R, \\ \frac{dS_L}{dt} &= \Delta\pi - (1 - q_1)(1 - a)S_L\lambda - q_3 S_L - \mu S_L + \theta\xi R, \\ \frac{dC}{dt} &= (1 - q_1)(S_H + (1 - a)S_L)\lambda - q_2\eta_2 C - (\sigma + \mu)C, \\ \frac{dI}{dt} &= \sigma C - q_2\eta_1 I - (\mu + d)I, \\ \frac{dR}{dt} &= q_3 S_H + q_2\eta_2 C + q_3 S_L + q_2\eta_1 I - (\theta\xi + (1 - \theta)\xi + \mu)R. \end{aligned} \tag{30}$$

The objective is to find the solution $(q_1^*(t), q_2^*(t), q_3^*(t))$ which minimizes the associated cost of vaccination, treatment, and personal protection (prevention). To balance the size of $C(t)$ and $I(t)$, we introduce the coefficients $Z_1 > 0$ and $Z_2 > 0$, which are linear, while the variables $D_1 > 0$, $D_2 > 0$, and $D_3 > 0$ are the associated weights of the cost of vaccination, treatment, and personal protection which take a quadratic form as explained in [32]. The quantity T_F in Equation (29) is the intervention time. Thus, $[0, T_F]$ is the given time interval in which we seek to minimize Equation (29). Hence, we use Pontryagin’s maximum principle applied in [33] to determine the necessary conditions that the optimal controls must satisfy. The Lagrangian and Ham-

iltonian are determined. The Lagrangian is given by

$$L(S_H, S_L, C, I, R, q_1, q_2, q_3) = \left(Z_1 C(t) + Z_2 I(t) + \frac{D_1}{2} q_1^2(t) + \frac{D_2}{2} q_2^2(t) + \frac{D_3}{2} q_3^2(t) \right). \tag{31}$$

We define the Hamiltonian, \mathcal{H} , to determine the minimum value of the Lagrangian as

$$\mathcal{H} = g(X_i(t), q_i(t)) + \sum_{i=1}^n \lambda_i X_i, \tag{32}$$

where

$$\begin{aligned} \mathcal{H} &= Z_1 C + Z_2 I + \frac{1}{2} (D_1 q_1^2 + D_2 q_2^2 + D_3 q_3^2) \\ &+ \lambda_{S_H} [(1 - \Delta)\pi - q_3 S_H - (1 - q_1)\lambda S_H - \mu S_H + (1 - \theta)\xi R] \\ &+ \lambda_{S_L} \left[\Delta\pi - (1 - q_1)(1 - a)S_L \frac{\beta(\omega C + \omega_1 I)}{N} - q_3 S_L - \mu S_L + \theta\xi R \right] \\ &+ \lambda_C \left[(1 - q_1)(S_H + (1 - a)S_L) \frac{\beta(\omega C + \omega_1 I)}{N} - q_2\eta_2 C - (\sigma + \mu)C \right] \\ &+ \lambda_I [\sigma C - q_2\eta_1 I - (\mu + d)I] + \lambda_R [q_3 S_H + q_2\eta_2 C + q_3 S_L + q_2\eta_1 I - (\theta\xi + (1 - \theta)\xi + \mu)R]. \end{aligned} \tag{33}$$

The parameters $\lambda_{S_H}, \lambda_{S_L}, \lambda_C, \lambda_I, \lambda_R$ in Equation (33) are the costate variables associated with the state variables $(S_H(t), S_L(t), C(t), I(t), R(t))$. To obtain the differential equations of the adjoint variables, we solve the partial derivatives of Equation (33) to the state variables and get

$$\begin{aligned} \frac{d\lambda_{S_H}}{dt} &= \lambda_{S_H}\mu + (\lambda_{S_H} - \lambda_R)q_3 + (\lambda_{S_H} - \lambda_C)(1 - q_1)(\beta(\omega C + \omega_1 I)) + (1 - \theta)\xi(\lambda_R - \lambda_{S_H}), \\ \frac{d\lambda_{S_L}}{dt} &= \lambda_{S_L}\mu + (\lambda_{S_L} - \lambda_R)q_3 + (\lambda_{S_L} - \lambda_C)(1 - q_1)(1 - a)(\beta(\omega C + \omega_1 I)) + (\lambda_R - \lambda_{S_L})\theta\xi, \\ \frac{d\lambda_C}{dt} &= -Z_1 + (\lambda_C - \lambda_R)q_2\eta_2 + \lambda_C\mu + (\lambda_C - \lambda_I)\sigma, \\ \frac{d\lambda_I}{dt} &= -Z_2 + (\lambda_I - \lambda_R)q_2\eta_1 + \lambda_I(\mu + d), \\ \frac{d\lambda_R}{dt} &= \lambda_R\mu + (\lambda_R - \lambda_{S_H})(1 - \theta)\xi + (\lambda_R - \lambda_{S_L})\theta\xi. \end{aligned} \tag{34}$$

Afterward, the standard existence result for minimizing a control problem as established in [32] is adapted as follows.

Theorem 4. *There exist optimal control variables q_1^*, q_2^*, q_3^* with the corresponding solutions S_H, S_L, C, I, R , which minimizes Equation (29) over Ω . Further, there exist costate variables satisfying the following:*

$$-\frac{d\lambda_i}{dt} = \frac{\partial \mathcal{H}}{\partial i}, \quad i \in \{S_H, S_L, C, I, R\}, \tag{35}$$

and the optimal solution (q_1^*, q_2^*, q_3^*) given by

$$\begin{aligned} q_1^* &= \min \{1, \max(0, \widehat{q}_1)\}, \\ q_2^* &= \min \{1, \max(0, \widehat{q}_2)\}, \\ q_3^* &= \min \{1, \max(0, \widehat{q}_3)\}. \end{aligned} \tag{36}$$

Proof. We find the control variables at critical points by considering the Hamiltonian equations:

$$\begin{aligned} \frac{\partial H}{\partial q_1} &= D_1 q_1 + (\lambda_{S_H} - \lambda_C(\beta * (\omega C + \omega_1 I)))S_H + (1 - a)(\lambda_{S_L} - \lambda_C)(\beta(\omega C + \omega_1 I))S_L = 0, \\ \frac{\partial H}{\partial q_2} &= D_2 q_2 + (\lambda_C - \lambda_R)\eta_2 C - (\lambda_I \lambda_R)\eta_1 I = 0, \\ \frac{\partial H}{\partial q_3} &= D_3 q_3 + (\lambda_{S_H} - \lambda_R)S_H + (\lambda_{S_L} - \lambda_R)S_L = 0. \end{aligned} \tag{37}$$

Taking the bounds of the control variables into consideration, we have

$$\begin{aligned} q_1^*(t) &= \min \left\{ \max \left\{ 0, \frac{(\lambda_C - \lambda_{S_H})(\beta(\omega C + \omega_1 I))S_H + (1 - a)(\lambda_C - \lambda_{S_L})(\beta(\omega C + \omega_1 I))S_L}{D_1} \right\}, 1 \right\}, \\ q_2^*(t) &= \min \left\{ \max \left\{ 0, \frac{(\lambda_R - \lambda_C)\eta_2 C + (\lambda_I - \lambda_R)\eta_1 I}{D_2} \right\}, 1 \right\}, \\ q_3^*(t) &= \min \left\{ \max \left\{ 0, \frac{(\lambda_R - \lambda_{S_H})S_H + (\lambda_R - \lambda_{S_L})S_L}{D_3} \right\}, 1 \right\}. \end{aligned} \tag{38}$$

TABLE 4: Estimated parameter values of system (2) obtained from the curve fitting process.

Parameter	Description	Value	Source
π	Recruitment rate	19787	Estimated
Δ	Individual's risk rate	0.585	Estimated
β	Effective contact rate	0-0.9	Estimated
ω	Per capita infection rate by carrier individuals	0.7420	[36, 37]
ω_1	Per capita infection rate by infected individuals	0-0.85	[37]
θ	Risk rate of individuals that loss immunity	0.6997	[37]
ξ	Loss of immunity	0.851	[37]
a	Modification rate	0.23	Estimated
σ	Rate of progression from C to I	0.00022	Estimated
d	Disease induce death rate	0.495	[23]
η_2	Recovery rate of carriers	0.8	Estimated/[23]
η_1	Recovery rate of infected individuals	0.43	Estimated/[23]
μ	Natural death rate	0.0152207	Estimated

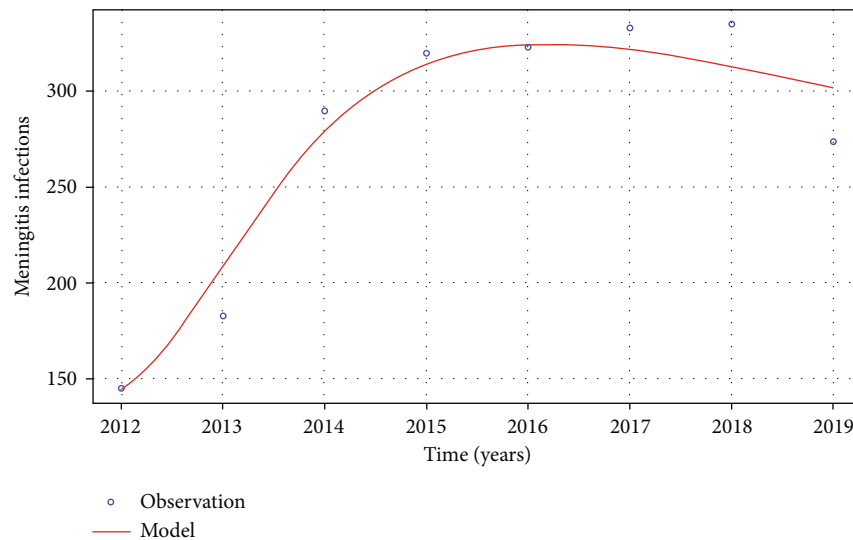


FIGURE 5: Fitted model of system (2) using the Nelder-Mead optimization approach. The least-squares regression or Nelder-Mead approach minimizes the mean of squared error (MSE) between the prediction states and their observation values from the data.

From Equation (38), we derive $\hat{q}_1, \hat{q}_2, \hat{q}_3$ as

$$\begin{aligned}
 \hat{q}_1 &= \frac{(\lambda_C - \lambda_{S_H})(\beta(\omega C + \omega_1 I))S_H + (1 - a)(\lambda_C - \lambda_{S_L})(\beta(\omega C + \omega_1 I)S_L)}{D_1}, \\
 \hat{q}_2 &= \frac{(\lambda_R - \lambda_C)\eta_2 C + (\lambda_I - \lambda_R)\eta_1 I}{D_2}, \\
 \hat{q}_3 &= \frac{(\lambda_R - \lambda_{S_H})S_H + (\lambda_R - \lambda_{S_L})S_L}{D_3}.
 \end{aligned}
 \tag{39}$$

□

4.1. *Parameter Estimation.* In this subsection, we estimate the parameter values in system (2) to derive the numerical

results from studying the extent and trend of meningitis infections in Ghana. We analyze the confirmed cases of meningitis infection recorded in the Upper West Region of Ghana from 2012 to 2019 obtained from the disease control unit at the Municipal Health Directorate under the Ghana Health Service (GHS) in the Upper West Region. Variables of interest were pulled out from the whole dataset and analyzed in R. The data obtained is publicly accessible, deidentified, and completely anonymised before use. Thus, we did not seek ethical approval because analysis of publicly accessible data without including personal information does not need ethical approval per current guidelines.

Fitting the model to data, we estimate the natural death rate (μ) as the inverse of life expectancy at birth. The natural

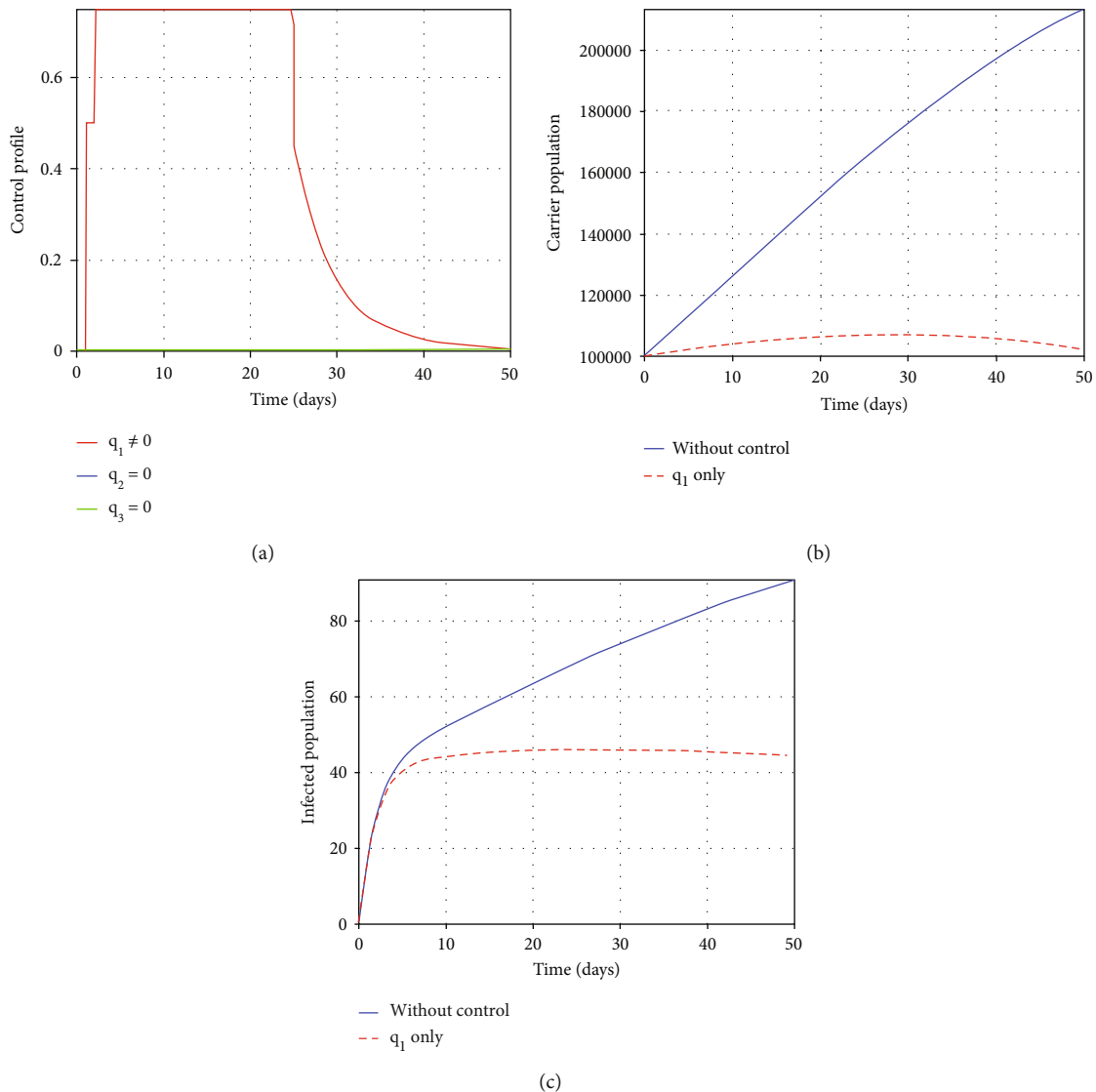


FIGURE 6: Effect of using vaccination only. The control profile associated with the use of vaccination only as an intervention measure in (a) indicates that health practitioners vaccinate about 50% of the population at risk with vaccination within two days and afterward increase the vaccination rate to cater for 80% of the population for 26 days to eradicate meningitis. Changes in the number of carriers in (b) and changes in the infected individuals in (c) show a decrease in these two groups when vaccination is applied.

death rate was calculated as $\mu = 0.0152207$ using Ghana’s average life expectancy of 65.7 years. Further, we estimate the state variables’ initial conditions using the Upper West Region’s demographic profile. For example, the total population of Upper West according to the 2021 census is about 1.3 million. Hence, given $N(t) = \pi/\mu$, we can estimate π as $\pi = \mu \times N(t) \approx 19787$. The remaining unknown parameter values were estimated using the Nelder-Mead optimization approach in [34]. The goal of the least-squares regression approach was to minimize the mean of squared error (MSE) between the prediction states and their observation values from the data retrieved. Equation (40) depicts the minimization of the sum of squared error between the model and data.

$$\min M(\rho) = \sum (Y(t, \rho) - X_r)^2, \quad (40)$$

where X_r is the actual or real reported data and $Y(t, \rho)$ denotes the solution of the model corresponding to the number of meningitis infections over time t and its corresponding set of estimated parameters represented by ρ .

We obtained the unknown parameter values implementing Equation (40) in R using deSolve and the FME package. Table 4 and Figure 5 show the parameter values and estimated model fit, respectively.

4.2. Numerical Results. In this subsection, we obtain appropriate results to ascertain the effect of the controls introduced in the system (2). We used the forward-backward sweep method (FBSM) and the Runge–Kutta 4th order numerical approach to solve the optimality of system (2) and perform the implementation using the Octave software (for a detailed description of the FBSM, see [35]). We used the parameter values in

Table 4 and the following values for the weights and state variables to obtain the numerical results.

$$\begin{aligned}
 Z_1 &= 10, \\
 Z_2 &= 25, \\
 D_1 &= 5, \\
 D_2 &= 25, \\
 D_3 &= 2, \\
 S_H &= 800000, \\
 S_L &= 300000, \\
 C &= 100000, \\
 I &= 0, \\
 R &= 99000.
 \end{aligned} \tag{41}$$

The following subsection describes the numerical results.

4.3. Strategy I: Application of a Single Control. This subsection investigates the effect of applying a single control as an intervention strategy to ascertain its effectiveness in reducing meningitis. The single controls are represented as intervention techniques by showing their respective control profile and the effect of applying single controls on the infectious compartments (carriers and infected population).

4.3.1. Intervention 1: Vaccination Only. The first single control strategy is to ascertain the application of vaccination only as an intervention technique. Vaccines are one of the most effective public health interventions in history, saving billions of lives since the first vaccine was produced in 1798 [38]. In the case of meningitis, meningococcal vaccines help protect against *N. meningitidis*. Figure 6 depicts the simulation results obtained when vaccination as the only intervention applied. Figure 6(a) depicts the control profile for applying only vaccination as a control technique. However, the blue line representing treatment (q_2) in Figure 6(a) is embedded in q_3 . Figure 6(a) depicts that if we seek to apply only vaccination as an intervention technique, one requires the health practitioners to vaccinate about 50% of the population at risk of meningitis infection within two days. Moreover, this number should be increased to about 80% and maintained for 26 days to eradicate meningitis and afterwards reduce or stop vaccinating at 50 days.

Figures 6(b) and 6(c) show that vaccination reduces the number of individuals with meningitis infections. The control profile (see Figure 6(a)) indicates that if 50% of individuals within the Upper West Region of Ghana receive vaccination within two days, the number of individuals regarded as carriers will begin to reduce after about six or eight days, thus, decreasing and stabilizing the number of people infected with meningitis, as shown in Figure 6(c). Hence, with this intervention technique, the result shown in Figure 6 for the infected compartments and the control profile indicates that vaccination is useful in minimizing meningitis infection.

4.3.2. Intervention 2: Treatment Only. Bacterial meningitis is contagious, caused by infection from certain bacteria. It is fatal if left untreated; hence, treatment is another primary intervention for reducing meningitis infection. Early diagnosis and treatment prevent brain damage and death [1]. From Figure 7(a), the control profile shows that one requires to treat about 15% of the population on the initial day of recording an individual infected with meningitis. Afterward, this should be increased to about 80% and maintained until health practitioners treat all carriers and infected individuals.

Figures 7(b) and 7(c) show the effect of applying treatment on both carrier and infected compartments, respectively. Both carrier and infected population reduce when we apply treatment compared with when treatment is not applied (see Figure 7(c)). However, after 40 days, we observed an increase in both carrier and infected individuals affirming the assertion by WHO and CDC that due to the several different causes and strains of meningitis, it is possible though rare, to have the disease more than once.

4.3.3. Intervention 3: Personal Protection Only. This intervention is achieved by setting $q_1 = q_2 = 0$ while $q_3 \neq 0$. An individual prevents meningitis when s/he observes the following protocols: restricting low-risk individuals from visiting specific locations such as the meningitis belt, especially during the dry season. Moreover, keeping distance, washing hands, and not sharing items where secretions can lurk, such as drinking glasses, water bottles, straws, silverware, toothbrushes, and cigarettes, can help reduce the spread of meningitis. The control profile of Figure 8(a) shows that about 100% of the individuals are required to apply personal protection techniques and maintain it for 12 days before the disease reduces to about 25% and is maintained for 25 days before it reduces to zero. We observe that personal protection techniques significantly reduce the number of infectious individuals, as shown in Figures 8(b) and 8(c).

The incubation period for meningitis is between 2 and 10 days. Figures 8(b) and 8(c) depict this scenario. We observe an initial increase in the infected but a reduction in the carrier population with personal protection as a control strategy, describing the incubation period. However, after about 2 to 8 days, there is a significant reduction in the number of infected individuals indicating that during this period, individuals that become carriers or move to the infected compartment duly observe the protocols required to recover.

4.4. Strategy II: Application of Two Controls. This subsection investigates the effect of applying two controls as an intervention strategy to ascertain its effectiveness in reducing meningitis. The two controls as intervention techniques are such that for intervention 4, $q_1 = q_2 \neq 0$ while $q_3 = 0$. Interventions 5 and 6 are denoted by $q_1 = q_3 \neq 0$ and $q_2 = 0$ and $q_2 = q_3 \neq 0$ and $q_1 = 0$, respectively. We show the respective control profiles and the effect of combining two controls on the infectious compartments (carriers and infected population).

4.4.1. Intervention 4: Vaccination and Treatment. Figure 9(a) shows that for vaccination and treatment to reduce the spread or transmission of meningitis effectively, the control q_1

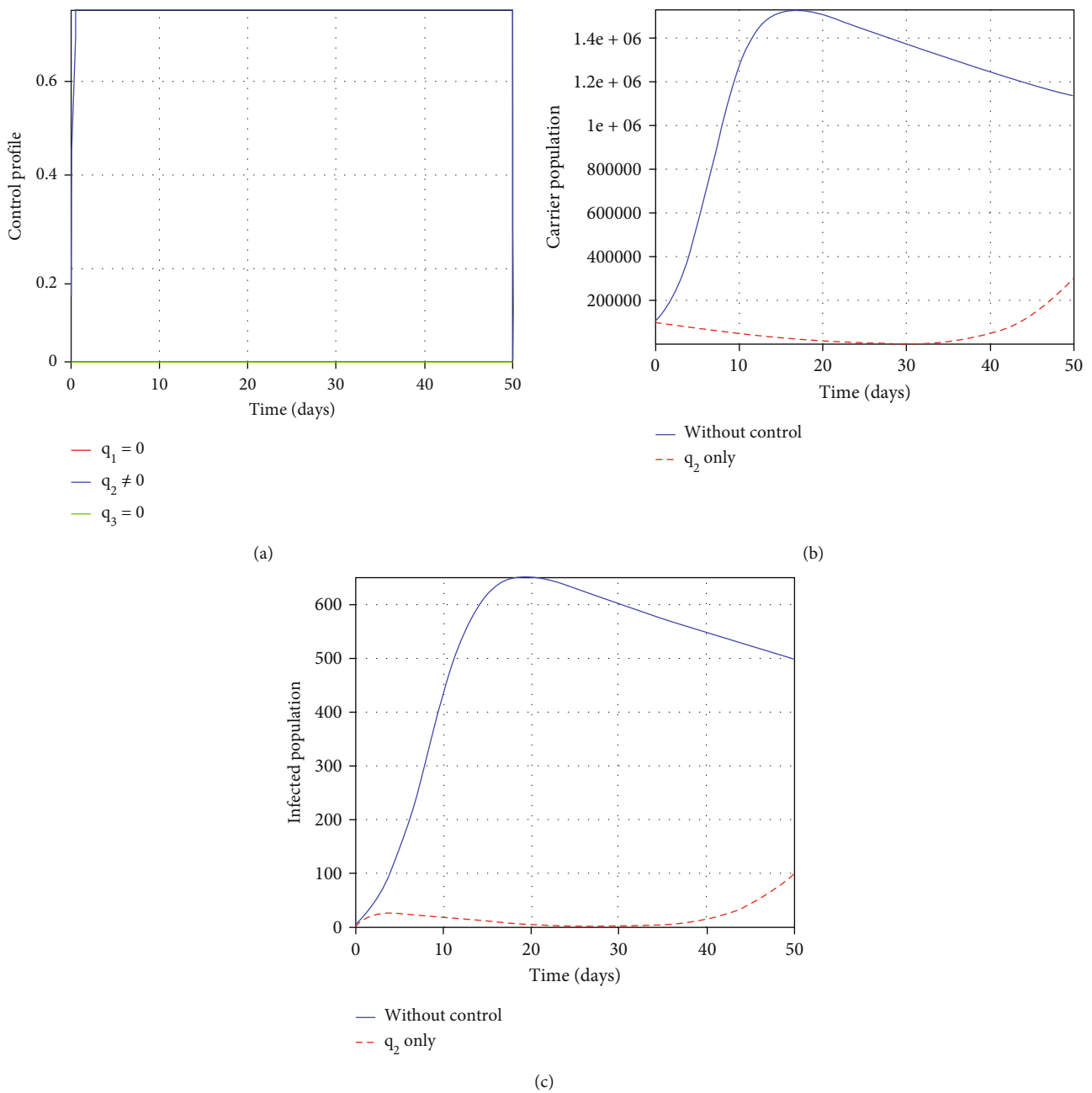


FIGURE 7: Effect of using treatment only. The control profile associated with the use of treatment as the only intervention measure in (a) shows that about 15% of the population with meningitis should be treated on the initial day and afterward 80% of these carriers and infected individuals be treated throughout the entire period. Changes in (b) carriers and (c) infected individuals show that incorporating treatment reduces the number of secondary infections in the population.

(vaccination) must be implemented throughout the 50 days, while we apply treatment for about 48 days. In light of this, Figures 9(b) and 9(c) show that the combined application of vaccination and treatment significantly impacts the number of infectious individuals. Furthermore, when compared to the case of the respective vaccination and treatment single control techniques, the combination of the two controls sets the system at a meningitis-free state at a shorter time frame for the carriers and asymptotically reduces the number of infected individuals.

4.4.2. *Intervention 5: Vaccination and Personal Protection.* Figure 10 depicts the behavior of applying vaccination and personal protection. The control profile (see Figure 10(a)) shows that, for these interventions to work perfectly, we must administer vaccination for about 50 days. However, because the incubation period of the bacteria is between 2 and 10 days, an individual will have to be effectively protected for about 14 days before such intervention can relapse. When we apply these timelines, we observe from Figures 10(b) and 10(c) that

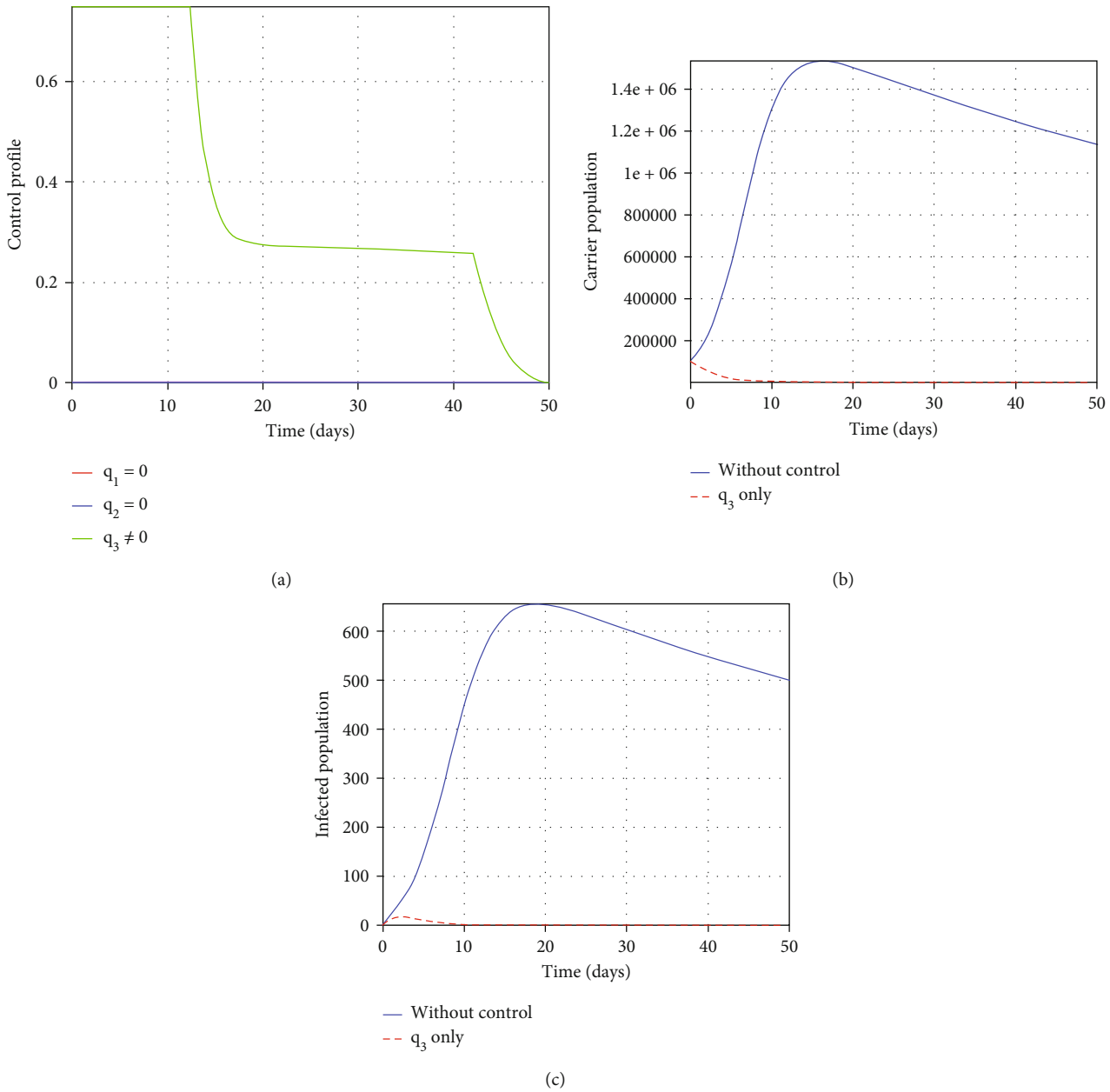


FIGURE 8: Effect of using personal protection only. The control graph in (a) clearly shows that 100% of the population is required to apply personal protection strategies and this should be done for 12 days to help eradicate the meningitis disease. The impact and effectiveness of this control strategy in averting the exponential growth in meningitis are seen in the decrease of (b) carriers and (c) infected individuals.

the number of carriers and infected individuals has reduced. Further, effective implementation of these combined intervention techniques quickly sets the system to a meningitis-free state compared to when we apply vaccination or personal protection as a single control strategy.

4.4.3. *Intervention 6: Treatment and Personal Protection.* Figure 11(a) represents the control profile at different values of q_2 and q_3 with $q_1 = 0$, while the rest of the plots that are Figures 11(b) and 11(c) denotes the effect of these controls on carriers and infected individuals, respectively. Figure 11(a) shows that 80% of the infected population must be treated to successfully eliminate meningitis. This should be accompanied

with an 80% of the carriers adhering to safe personal protection practices. Afterward, these numbers must then be kept for the duration of the epidemic period. The effective implementation of these interventions leads to a reduction in the number of individuals within the carrier and infected compartments, shown in Figures 11(b) and 11(c) (as shown by the red dotted lines). Moreover, when most infected individuals receive treatment, the system settles at a meningitis-free state (see Figure 11(c)). Also, it was observed that the carrier compartment (see Figure 11(b)) also settles at the meningitis-free state after 8 days affirming the stated incubation period in adhering to the strategy of practicing personal protection).

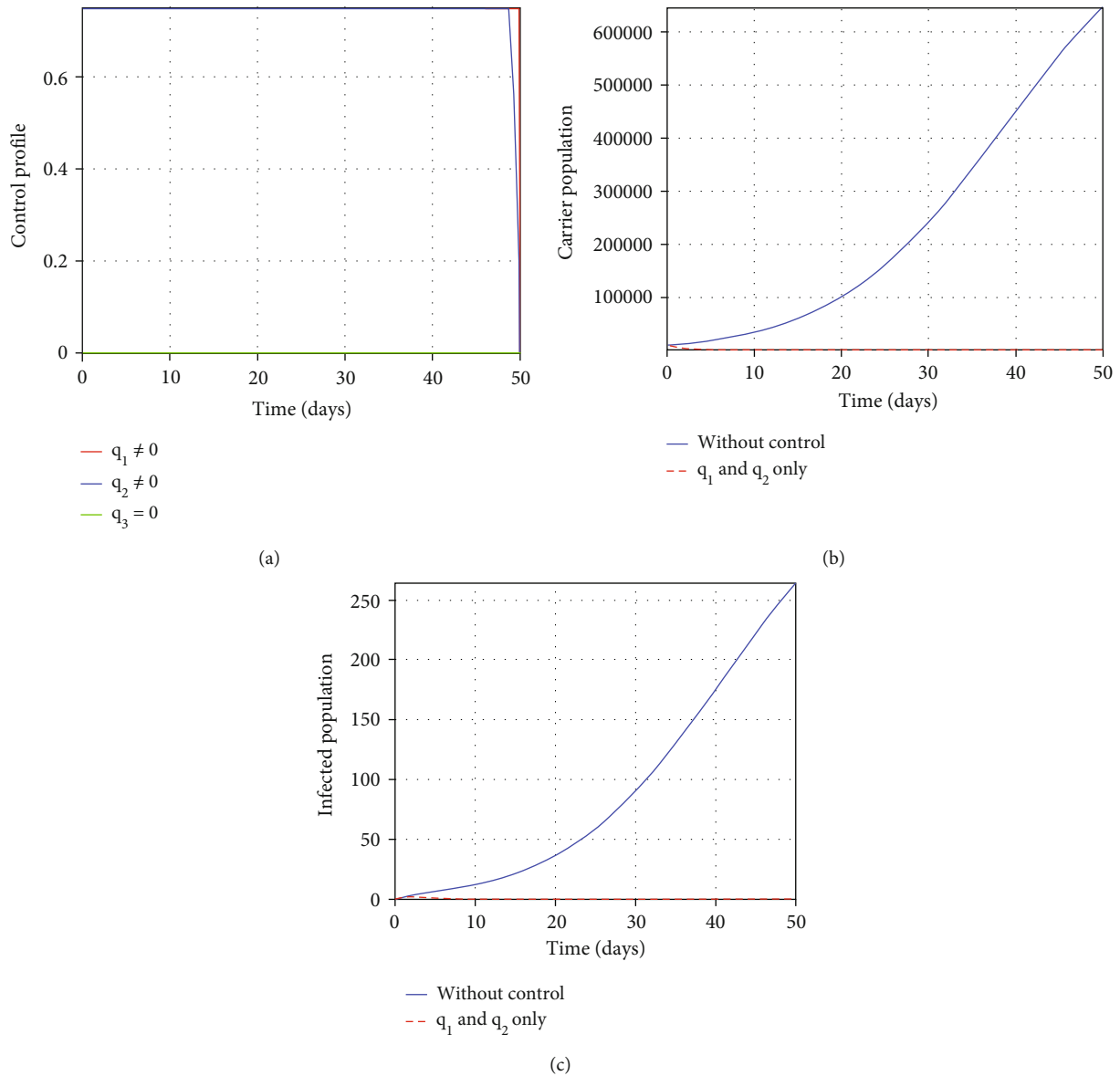


FIGURE 9: Effect of using both vaccination and treatment only. The control profile in (a) shows that for effective eradication of meningitis, vaccination must be applied to all individuals for 50 days while treatment is implemented for 48 days. The simulation result of the optimal control model shows the effectiveness of these measures on (b) carriers and (c) infected individuals. In the graphs, the solid line denotes without the strategy while dotted line indicates implementation of the control strategy.

4.5. *Strategy III: Application of All Controls.* This subsection investigates the effect of applying all the controls introduced in the article as an intervention strategy to ascertain its effectiveness in reducing meningitis. We denote the case where the controls are applied as $q_1 = q_2 = q_3 \neq 0$ and the situation without controls by $q_1 = q_2 = q_3 = 0$. Furthermore, we present their respective control profile and the effect of combining the three controls on the infectious compartments (carriers and infected population).

4.5.1. *Intervention 7: Vaccination, Treatment, and Personal Protection.* Figure 12(a) shows the control profile of applying all three controls. It further depicts that all controls be maintained at about 80% for about 46 days for personal protection, 47 days for treatment, and 50 days for vaccination. For personal

protection, this strategy can be reduced to about 30% after 46 days while maintaining treatment and vaccination at 100%. Thus, Figures 12(b) and 12(c) show that when we implement these strategies, they will reduce the spread of meningitis by both carriers and infected individuals. It further indicates that the disease settles at a meningitis-free state after the set incubation period of 10 days.

4.6. *Cost-Effectiveness Analysis.* Using cost-effectiveness analysis (CEA), researchers seek to compare one or more costs of interventions and health outcomes [39]. CEA gives information on an intervention's health and economic consequences compared to an alternative intervention. An intervention's cost-effectiveness ratio is calculated when the net costs of the intervention are positive (which indicates that a more effective

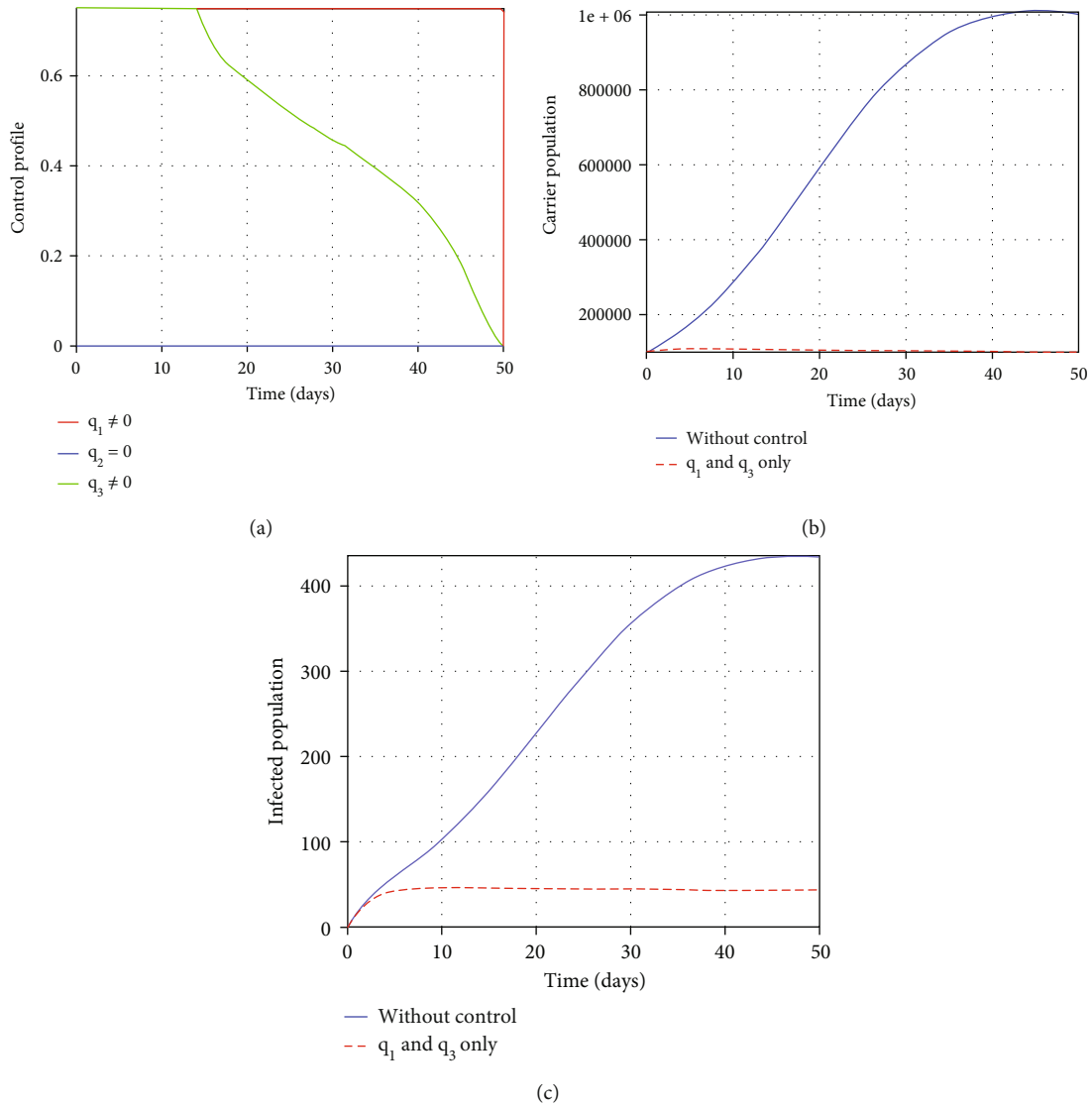


FIGURE 10: Effect of using both vaccination and personal protection only. The simulation results of the control profile in (a) show the effectiveness of this strategy. To eradicate meningitis, vaccination must be administered for all individuals throughout the period while personal protection is encouraged for at least 14 days during the period of infectiousness. The simulation result of the optimal control model shows the effectiveness of these measures on (b) carriers and (c) infected individuals. In the graphs, solid line denotes without control while dotted line indicates implementation of the controls.

intervention is more expensive). Net costs divided by changes in health outcomes are defined as the cost-effectiveness ratio [40, 41]. Using CEA to compare the health and cost consequences of several control measures that influence the same health outcome is valuable.

Additionally, it becomes beneficial in determining the intervention cost concerning the amount of health outcome achieved. Thus, decision-makers may benefit from knowing

whether or not an intervention is cost-effective, which helps to avoid the dissipation of limited resources. We use the objective function in Equation (29) to derive the total cost for each single and combined intervention measure. At the same time, we obtain the infection averted by calculating the difference between infectious individuals with and without the control measures. Table 5 depicts the result of meningitis infection averted (MIA) and the total cost (TC).

$$ICER = \frac{\text{Change in total costs between control measures}}{\text{Change in total number of infections averted between control measures}} \quad (42)$$

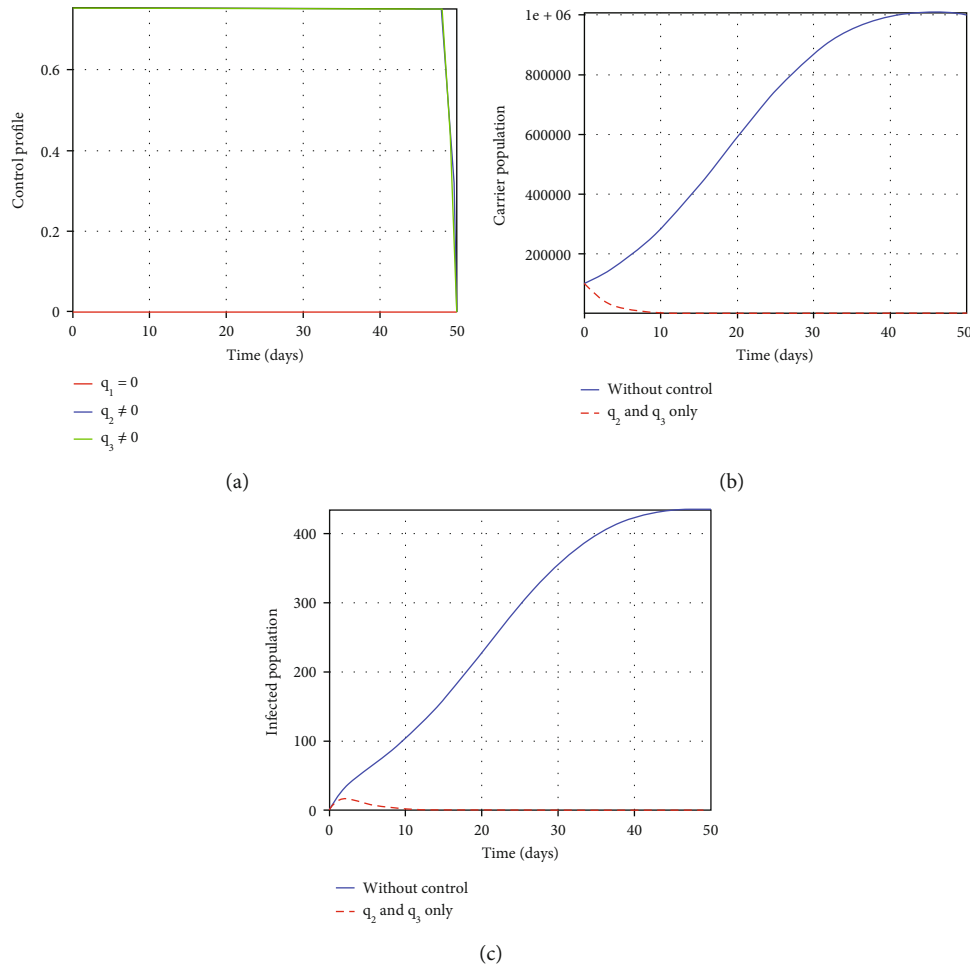


FIGURE 11: Effect of using both treatment and personal protection only. The control profile in (a) shows the impact of early treatment and adherence of personal protection techniques in the population. About 80% of individuals are required to receive treatment and personally protect themselves to help eradicate the meningitis disease. The graphs clearly show the impact and effectiveness of both treatment and personal protection in averting the number of (b) carriers and (c) infected individuals.

According to [42], the incremental cost-effectiveness ratio (ICER) explains the cost-effectiveness analysis. ICER is used to

We rank the MIA in increasing order of effectiveness, and by using Equation (42), we calculate the ICER ratio for the various interventions (I) as follows:

$$\begin{aligned}
 ICER(I3) &= \frac{4.253}{5305486.76251} = 8.016 \times 10^{-7}, \\
 ICER(I1) &= \frac{(12.517 - 4.253)}{(5307317.89534 - 5305486.76251)} = 4.513 \times 10^{-3}, \\
 ICER(I5) &= \frac{(16.770 - 12.517)}{(5308148.18249 - 5307317.89534)} = 5.122 \times 10^{-3}, \\
 ICER(I2) &= \frac{(12.500 - 16.770)}{(5309044.53425 - 5308148.18249)} = -4.76 \times 10^{-3}, \\
 ICER(I6) &= \frac{(16.753 - 12.500)}{(5309873.63189 - 5309044.53425)} = 5.130 \times 10^{-3}, \\
 ICER(I4) &= \frac{(25.017 - 16.753)}{(5311683.62738 - 5309873.63189)} = 4.566 \times 10^{-3}, \\
 ICER(I7) &= \frac{(29.270 - 25.017)}{(5312501.97405 - 5311683.62738)} = 5.197 \times 10^{-3}.
 \end{aligned}
 \tag{43}$$

explore any two competing measures or interventions for controlling the spread of disease. The ICER formula is given as

In what follows, Table 6 summarizes the ICER for each interventions based on the increasing rank order of effectiveness for the meningitis infection averted cases by the interventions employed in the study.

It is revealed in Table 6 that between interventions 3 and 1, we incur an additional cost of 8.016×10^{-7} when we implement personal protection only as a control measure compared to the extra cost of 4.513×10^{-3} incurred when vaccination only is applied. Thus, $I1$ is more expensive and less effective than $I3$. Hence, we exclude $I1$ from the list of alternative control measures competing for the same limited resources. For this reason, we recalculate the ICER for $I3$ and $I5$. The result is shown in Table 7.

From Table 7, an asterisk (*) behind an intervention shows the comparing items under consideration. After recalculating the ICER value, the observation indicates that intervention 5 was expensive and less effective to implement than 3. Hence, we exclude intervention 5 from the list of considered

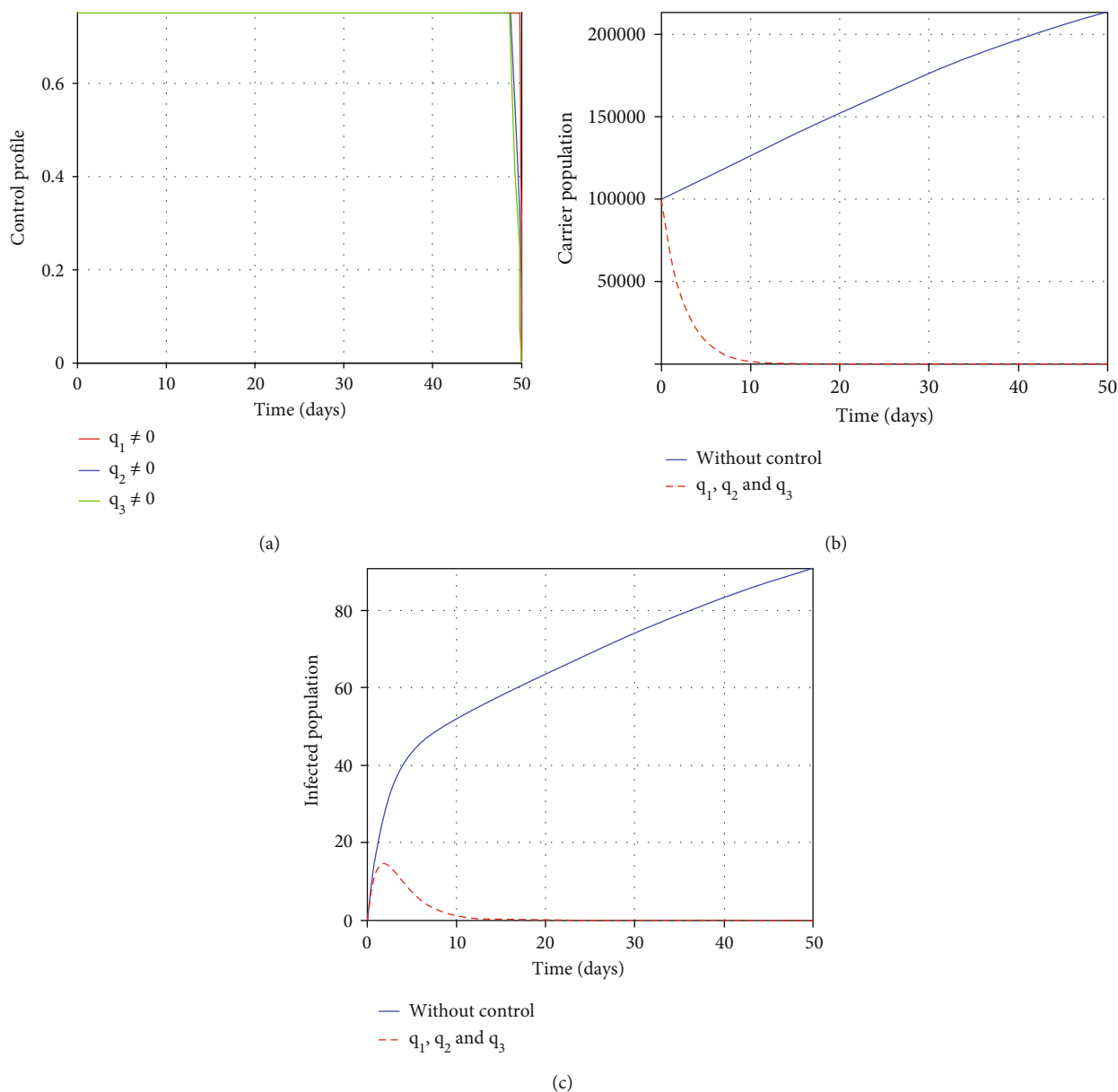


FIGURE 12: Effect of using all controls: vaccination, treatment, and personal protection. For effective meningitis eradication, 80% of individuals must personally protect themselves for 46 days while treatment and vaccination must be implemented for 47 and 50 days, respectively, as shown by the control profile in (a). The graphs clearly show the impact and effectiveness in averting the number of (b) carriers and (c) infected individuals.

TABLE 5: Meningitis infection averted and total cost for the various control measures.

Strategy	Intervention	Control measures	MIA	TC
I	1	Vaccination only	5307317.89534	\$12.517
	2	Treatment only	5309044.53425	\$12.500
	3	Personal protection only	5305486.76251	\$4.253
II	4	Vaccination and treatment	5311683.62738	\$25.017
	5	Vaccination and personal protection	5308148.18249	\$16.770
	6	Treatment and personal protection	5309873.63189	\$16.753
III	7	Vaccination, treatment, and personal protection	5312501.97405	\$29.270

TABLE 6: ICER ratio based on increasing order of meningitis infection averted (MIA) and its associated cost (TC) for each intervention.

Intervention	Control measure	MIA	TC	ICER
3	Personal protection only	5305486.76251	\$4.253	8.016×10^{-7}
1	Vaccination only	5307317.89534	\$12.517	4.513×10^{-3}
5	Vaccination and personal protection	5308148.18249	\$16.770	5.122×10^{-3}
2	Treatment only	5309044.53425	\$12.500	-4.764×10^{-3}
6	Treatment and personal protection	5309873.63189	\$16.753	5.130×10^{-3}
4	Vaccination and treatment	5311683.62738	\$25.017	3.351×10^{-3}
7	Vaccination, treatment, and personal protection	5312501.97405	\$29.270	5.197×10^{-3}

TABLE 7: Comparing ICER I_3 with I_5 .

Intervention	Control measure	MIA	TC	ICER
3*	Personal protection only	5305486.76251	\$4.253	8.016×10^{-7}
5*	Vaccination and personal protection	5308148.18249	\$16.770	4.703×10^{-3}
2	Treatment only	5309044.53425	\$12.500	-4.764×10^{-3}
6	Treatment and personal protection	5309873.63189	\$16.753	5.130×10^{-3}
4	Vaccination and treatment	5311683.62738	\$25.017	3.351×10^{-3}
7	Vaccination, treatment, and personal protection	5312501.97405	\$29.270	5.197×10^{-3}

TABLE 8: Comparing ICER I_3 with I_2 .

Intervention	Control measure	MIA	TC	ICER
3*	Personal protection only	5305486.76251	\$4.253	8.016×10^{-7}
2*	Treatment only	5309044.53425	\$12.500	2.318×10^{-3}
6	Treatment and personal protection	5309873.63189	\$16.753	5.130×10^{-3}
4	Vaccination and treatment	5311683.62738	\$25.017	3.351×10^{-3}
7	Vaccination, treatment, and personal protection	5312501.97405	\$29.270	5.197×10^{-3}

TABLE 9: Comparing ICER I_3 with I_6 .

Intervention	Control measure	MIA	TC	ICER
3*	Personal protection only	5305486.76251	\$4.253	8.016×10^{-7}
6*	Treatment and personal protection	5309873.63189	\$16.753	5.130×10^{-3}
4	Vaccination and treatment	5311683.62738	\$25.017	2.849×10^{-3}
7	Vaccination, treatment, and personal protection	5312501.97405	\$29.270	5.197×10^{-3}

TABLE 10: Comparing ICER I_3 with I_4 .

Intervention	Control measure	MIA	TC	ICER
3*	Personal protection only	5305486.76251	\$4.253	8.016×10^{-7}
4*	Vaccination and treatment	5311683.62738	\$25.017	6.915×10^{-3}
7	Vaccination, treatment, and personal protection	5312501.97405	\$29.270	5.197×10^{-3}

TABLE 11: Comparing ICER *I3* with *I7*.

Intervention	Control measure	MIA	TC	ICER
3*	Personal protection only	5305486.76251	\$4.253	8.016×10^{-7}
7*	Vaccination, treatment, and personal protection	5312501.97405	\$29.270	5.197×10^{-3}

alternative interventions. As such, we recalculate and compare the effect between interventions 3 and 2 (see Table 8).

Comparing intervention 3 with 2, we observed that it was more cost-effective to implement intervention 3 than 2. Hence, we exclude 2 from the list and proceed to compare 3 with 6.

Table 9 indicates that implementing personal protection as an intervention for the control of meningitis is effective and less costly compared with *I6*. Implementing *I3* only adds a cost of 8.016×10^{-7} , but that of *I6* poses an additional cost of 5.130×10^{-3} . Hence, we exclude *I6* from the comparative list and further assess it by comparing *I3* with *I4* (see Table 10).

Comparing intervention 3 with 4, as shown in Table 10, indicates that intervention 4 is more costly and less effective than *I3*. Therefore, we exclude *I4* and finally compare *I3* with *I7*.

The final comparative analysis between interventions 3 and 7, as shown in Table 11, revealed that *I7* is more costly and less effective. Thus, we exclude *I7*. Consequently, implementing intervention 3 is the most cost-effective strategy among the seven interventions considered in this paper.

5. Discussions and Conclusion

According to [43], one of the most preventable measures of meningitis is mostly through vaccination and treatment. Still, progress in the fight against the disease through these measures is behind other diseases that are preventable by vaccination and treatment. Moreover, the economic burden reported in [13] from the societal perspective showed that the northern part of Ghana, with a total population of about 5,068,521, spent \$5,230,035 per year (\$777 per case) on meningitis management. Regarding age composition, [13] indicated that the cost per meningitis vaccination or treatment for children under five years was \$2,128, \$3,247 for children between 5 and 14 years, and \$2,883 for individuals who are 15 years and above.

The result from [13] shows that the economic burden of meningitis disease in northern Ghana remains substantial, especially in older children and adults who we expect to have benefited from indirect effects because they received infant immunization. The costly nature of vaccination and treatment, as affirmed in this article from the cost-effectiveness analysis result in Table 11, shows that the most cost-effective approach the government of Ghana should implement is to encourage personal protection. Personal protection is important because bacterial meningitis often spreads through droplets from the mouth or nose. Therefore, individuals must take precautions to prevent the spread of these droplets. Most individuals acquire meningococcal disease through exposure to asymptomatic carriers. Hence, if we do not include low-risk individuals in epidemic models, the projected contribution of the high-risk groups,

and thus, the potential impact of prioritizing interventions to address their needs, could be underestimated. We would like to point out that the goal was to look at the optimal and cost-effective strategies designed to help policymakers keep the total infected population at a minimum, considering the effects of the high- and low-risk population proportions. Another important factor that we did not implement in this work, the role of mobility among high- and low-risk individuals, is being considered in follow-up work. Thus, we now sum up our study in the next paragraph.

In this study, we discuss the dynamics of meningitis infection in Ghana using a mathematical model incorporating the behavior of high- and low-risk individuals. The proposed model allows for the possible transmission of infection from low-risk individuals under certain conditions. The movement of individuals from the carrier stage to the infected stage depends on the activities they engage in, which the basic reproduction number depicts in Equation (16), such that for $\sigma = 0$, there is no progression to the infected compartment. The asymptotic behaviors of system 2 were determined using the basic reproductive number. The system exhibited a meningitis-free state when $R_0 < 1$ and a backward bifurcation scenario where a stable MFE coexists with a stable endemic existence for $R_0 < 1$. Thus, by implication, controlling the disease lies in the initial conditions. The time-dependent basic reproductive number was sensitive to the choice of generation time of the infection. Thus, we designed an optimal control problem that minimizes the cost of implementation of the controls while also minimizing the total number of infected individuals over the intervention interval. First, we demonstrated that the optimal control exists and portrayed it in terms of the solution to the optimality system.

Additionally, we established that the control system must be unique for a sufficient time frame to find the optimality. We use Pontryagin's maximum principle to find necessary conditions for the optimal values of the controls that minimize the spread of meningitis together with the cost of implementing the controls or interventions. The ICER was used to assess the most effective intervention among the seven interventions employed. Though controlling meningitis intensely relies on treatment in the Ghanaian context, this article showed that encouraging and implementing personal protection can provide the most cost-effective method of controlling meningitis.

Other future investigations based on the obtained results will concern transforming the present integer-based model to a fractional order model incorporating a dataset that takes into consideration the whole meningitis belt of Ghana.

Data Availability

The data supporting this research are publicly available on the Ghana Health Service website which can be easily accessed.

Conflicts of Interest

The authors declare that they have no conflicts of interest.

Acknowledgments

This research was supported by the Fogarty International Center (FIC) and National Institute of Health with grant number U2RTW010679.

References

- [1] A. M. Oordt-Speets, R. Bolijn, R. C. van Hoorn, A. Bhavsar, and M. H. Kyaw, "Global etiology of bacterial meningitis: a systematic review and meta-analysis," *PLoS One*, vol. 13, no. 6, article 0198772, 2018.
- [2] M. Ceyhan, Y. Ozsurekci, S. Tanir Basaranoglu et al., "Multi-center hospital-based prospective surveillance study of bacterial agents causing meningitis and seroprevalence of different serogroups of neisseria meningitidis, haemophilus influenzae type b, and streptococcus pneumoniae during 2015 to 2018 in Turkey," *MSphere*, vol. 5, no. 2, p. 00060, 2020.
- [3] D. S. Stephens, B. Greenwood, and P. Brandtzaeg, "Epidemic meningitis, meningococcaemia, and *Neisseria meningitidis*," *The Lancet*, vol. 369, no. 9580, pp. 2196–2210, 2007.
- [4] M. A. Ward, T. M. Greenwood, D. R. Kumar, J. J. Mazza, and S. H. Yale, "Josef Brudzinski and Vladimir Mikhailovich Kernig: signs for diagnosing meningitis," *Clinical Medicine & Research*, vol. 8, no. 1, pp. 13–17, 2010.
- [5] G. Amarilyo, A. Alper, A. Ben-Tov, and G. Grisaru-Soen, "Diagnostic accuracy of clinical symptoms and signs in children with meningitis," *Pediatric Emergency Care*, vol. 27, no. 3, pp. 196–199, 2011.
- [6] D. Swanson, "Meningitis," *Pediatrics in review*, vol. 36, no. 12, pp. 514–526, 2015.
- [7] F. Simon, J.-P. Boutin, J.-M. Milleliri, and J.-N. Tournier, "Cerebrospinal meningitis: lessons learnt from Africa," *The Lancet Infectious Diseases*, vol. 19, no. 10, p. 1056, 2019.
- [8] S. Mazamay, J.-F. Guégan, N. Diallo et al., "An overview of bacterial meningitis epidemics in Africa from 1928 to 2018 with a focus on epidemics "outside-the-belt,"" *BMC Infectious Diseases*, vol. 21, no. 1, pp. 1–13, 2021.
- [9] M. Shirber, *Climate Conditions Help Forecast Meningitis Outbreaks*, 2014, <https://climate.nasa.gov/news/1054/climate-conditions-help-forecast-meningitis-outbreaks/>.
- [10] J. Leimkugel, A. Hodgson, A. A. Forgor et al., "Clonal waves of *Neisseria* colonisation and disease in the African meningitis belt: eight-year longitudinal study in northern Ghana," *PLoS Medicine*, vol. 4, no. 3, p. 101, 2007.
- [11] S. N. A. Codjoe and V. A. Nabie, "Climate change and cerebrospinal meningitis in the Ghanaian meningitis belt," *International Journal of Environmental Research and Public Health*, vol. 11, no. 7, pp. 6923–6939, 2014.
- [12] C. H. Bozio, A. Abdul-Karim, J. Abenyeri et al., "Continued occurrence of serotype 1 pneumococcal meningitis in two regions located in the meningitis belt in Ghana five years after introduction of 13-valent pneumococcal conjugate vaccine," *PLoS One*, vol. 13, no. 9, article 0203205, 2018.
- [13] M. Kobayashi, A. Abdul-Karim, J. L. Milucky et al., "Estimating the economic burden of pneumococcal meningitis and pneumonia in northern Ghana in the African meningitis belt post-PCV13 introduction," *Vaccine*, vol. 39, no. 33, pp. 4685–4699, 2021.
- [14] T. Letsa, C. L. Noora, G. K. Kuma et al., "Pneumococcal meningitis outbreak and associated factors in six districts of Brong Ahafo region, Ghana, 2016," *BMC Public Health*, vol. 18, no. 1, pp. 1–10, 2018.
- [15] B. B. Kaburi, C. Kubio, E. Kenu et al., "Evaluation of the enhanced meningitis surveillance system, Yendi municipality, northern Ghana, 2010–2015," *BMC Infectious Diseases*, vol. 17, no. 1, pp. 1–11, 2017.
- [16] A. Wilder-Smith, "Meningococcal disease: risk for international travellers and vaccine strategies," *Travel Medicine and Infectious Disease*, vol. 6, no. 4, pp. 182–186, 2008.
- [17] A. Pavli, P. Katerelos, P. Smeti, and H. C. Maltezou, "Meningococcal vaccination for international travellers from Greece visiting developing countries," *Travel Medicine and Infectious Disease*, vol. 14, no. 3, pp. 261–266, 2016.
- [18] C. P. García-Pando, M. C. Thomson, M. C. Stanton et al., "Meningitis and climate: from science to practice," *Earth Perspectives*, vol. 1, no. 1, pp. 14–15, 2014.
- [19] N. Young and M. Thomas, "Meningitis in adults: diagnosis and management," *Internal Medicine Journal*, vol. 48, no. 11, pp. 1294–1307, 2018.
- [20] F. Y. Aku, F. C. Lessa, F. Asiedu-Bekoe et al., "Meningitis outbreak caused by vaccine-preventable bacterial pathogens—northern Ghana, 2016," *MMWR. Morbidity and Mortality Weekly Report*, vol. 66, no. 30, pp. 806–810, 2017.
- [21] A. Karachaliou, A. J. Conlan, M.-P. Preziosi, and C. L. Trotter, "Modeling long-term vaccination strategies with menafriovac in the African meningitis belt," *Clinical Infectious Diseases*, vol. 61, Supplement 5, pp. 594–600, 2015.
- [22] I. M. Elmojtaba and S. O. Adam, "A mathematical model for meningitis disease," *Red Sea University Journal of Basic and Applied Science*, vol. 2, no. 2, pp. 467–472, 2017.
- [23] J. K. K. Asamoah, F. Nyabadza, B. Seidu, M. Chand, and H. Dutta, "Mathematical modelling of bacterial meningitis transmission dynamics with control measures," *Computational and Mathematical Methods in Medicine*, vol. 2018, Article ID 2657461, 21 pages, 2018.
- [24] I. A. Baba, L. I. Olamilekan, A. Yusuf, and D. Baleanu, "Analysis of Meningitis Model: A Case Study of Northern Nigeria," *AIMS Bioengineering*, vol. 7, no. 4, pp. 179–193, 2020.
- [25] J. K. K. Asamoah, F. Nyabadza, Z. Jin et al., "Backward bifurcation and sensitivity analysis for bacterial meningitis transmission dynamics with a nonlinear recovery rate," *Chaos, Solitons & Fractals*, vol. 140, article 110237, 2020.
- [26] World Health Organization, *Defeating Meningitis by 2030: A Global Road Map*, 2021.
- [27] J. M. Mwenda, E. Soda, G. Weldegebriel et al., "Pediatric bacterial meningitis surveillance in the world health organization African region using the invasive bacterial vaccine-preventable disease surveillance network, 2011–2016," *Clinical Infectious Diseases*, vol. 69, Supplement 2, pp. 49–57, 2019.
- [28] P. L. Delamater, E. J. Street, T. F. Leslie, Y. T. Yang, and K. H. Jacobsen, "Complexity of the basic reproduction number (R_0)," *Emerging Infectious Diseases*, vol. 25, no. 1, pp. 1–4, 2019.
- [29] D. Breda, T. Kuniya, J. Ripoll, and R. Vermiglio, "Collocation of next-generation operators for computing the basic

- reproduction number of structured populations,” *Journal of Scientific Computing*, vol. 85, no. 2, pp. 1–33, 2020.
- [30] J. Ma, “Estimating epidemic exponential growth rate and basic reproduction number,” *Infectious Disease Modelling*, vol. 5, pp. 129–141, 2020.
- [31] T. Obadia, R. Haneef, and P.-Y. Boëlle, “The R0 package: a toolbox to estimate reproduction numbers for epidemic outbreaks,” *BMC Medical Informatics and Decision Making*, vol. 12, no. 1, pp. 1–9, 2012.
- [32] N. K.-D. O. Opoku and C. Afriyie, “The role of control measures and the environment in the transmission dynamics of cholera,” *Abstract and Applied Analysis*, vol. 2020, Article ID 2485979, 16 pages, 2020.
- [33] L. S. Pontryagin, *Mathematical Theory of Optimal Processes*, Gordon and Breach Science Publishers, 1987.
- [34] S. Singer and J. Nelder, “Nelder-mead algorithm,” *Scholarpedia*, vol. 4, no. 7, p. 2928, 2009.
- [35] M. McAsey, L. Mou, and W. Han, “Convergence of the forward-backward sweep method in optimal control,” *Computational Optimization and Applications*, vol. 53, no. 1, pp. 207–226, 2012.
- [36] K. Vereen, *An Scir Model of Meningococcal Meningitis*, Virginia Commonwealth University, 2008.
- [37] T. Irving, K. Blyuss, C. Colijn, and C. Trotter, “Modelling meningococcal meningitis in the african meningitis belt,” *Epidemiology & Infection*, vol. 140, no. 5, pp. 897–905, 2012.
- [38] C. Rodrigues and S. A. Plotkin, “Impact of vaccines; health, economic and social perspectives,” *Frontiers in Microbiology*, vol. 11, p. 1526, 2020.
- [39] F. Agosto and M. Leite, “Optimal control and cost-effective analysis of the 2017 meningitis outbreak in Nigeria,” *Infectious Disease Modelling*, vol. 4, pp. 161–187, 2019.
- [40] J. K. K. Asamoah, Z. Jin, and G.-Q. Sun, “Non-seasonal and seasonal relapse model for q fever disease with comprehensive cost-effectiveness analysis,” *Results in Physics*, vol. 22, article 103889, 2021.
- [41] S. Olaniyi, O. Obabiyi, K. Okosun, A. Oladipo, and S. Adewale, “Mathematical modelling and optimal cost-effective control of COVID-19 transmission dynamics,” *The European Physical Journal Plus*, vol. 135, no. 11, p. 938, 2020.
- [42] N. K.-D. O. Opoku, G. Bader, and E. Fiatsonu, “Controlling crime with its associated cost during festive periods using mathematical techniques,” *Chaos, Solitons & Fractals*, vol. 145, article 110801, 2021.
- [43] F. Dejongh, “New global meningitis strategy aims to save 200,000 lives a year,” 2021, <https://news.un.org/en/story/2021/09/1101352>.